sustainability

MDPI

Article

Modeling Impact of Transportation Infrastructure-Based Accessibility on the Development of Mixed Land Use Using Deep Neural Networks: Evidence from Jiang'an District, City of Wuhan, China

Yunes Almansoub [1,2,3], Ming Zhong [1,2], Muhammad Safdar [1,2,*], Asif Raza [4], Abdelghani Dahou [5] and Mohammed A. A. Al-qaness [6,7]

1 Intelligent Transport Systems Research Center, Wuhan University of Technology, Wuhan 430063, China; almansoob@whut.edu.cn (Y.A.); mzhong@whut.edu.cn (M.Z.)
2 National Engineering Research Center for Water Transport Safety, Engineering Research Center for Transportation Safety, Wuhan 430063, China
3 Faculty of Computer Science and IT, Al-Razi University, Sana'a 12544, Yemen
4 College of Civil Aviation, Nanjing University of Aeronautics and Astronautics (NUAA), Nanjing 211106, China; asifraza@nuaa.edu.cn
5 L.D.D.I. Laboratory, Faculty of Science and Technology, University of Ahmed DRAIA, Adrar 01000, Algeria; dahou.abdghani@univ-adrar.edu.dz
6 College of Physics and Electronic Information Engineering, Zhejiang Normal University, Jinhua 321004, China; alqaness@zjnu.edu.cn
7 College of Engineering and Information Technology, Emirates International University, Sana'a 16881, Yemen
* Correspondence: safdar@whut.edu.cn

Abstract: Mixed land use (MLU) plays a crucial role in fostering a sustainable urban development, vibrant communities, and efficient land utilization, providing a viable solution for smart growth, inclusive public transit, and urban sustainability. This study employs deep neural network (DNN) models: multilayer perceptron (MLP), and long short-term memory (LSTM), to analyze the effect of the transportation infrastructure-based accessibility on the prevalence of MLU patterns, based on the following data: infrastructure-based accessibility measures represented by the logsum (or transport supply), MLU patterns at the parcel level, and floor space prices by space type, for the years 2012 and 2015. Furthermore, the proposed methods are applied to the Jiang'an District of the city of Wuhan, China, at the parcel level as the case study. The study results reveal that MLU is predominantly accessible in areas close to the city center, characterized by a high density, and is relatively scarce on the city outskirts. Notably, parcels exhibiting mixed residential–commercial and residential land-use patterns underwent significant changes between 2012 and 2015, particularly in regions with robust accessibility via non-motorized modes and public transit, specifically in the central and southern parts of Jiang'an District. This transition is evident under scenario 3 (walk, bike, bus, subway) and scenario 6 (walk, bus, car) considered in this study. Furthermore, the study observed a substantial expansion in mixed commercial–residential and commercial districts, significantly near the high-transit accessibility area of subway line 1, as demonstrated in scenario 7 (bike, subway, taxi). The results from the MLP models show a mean relative error (MRE) of 4.7–14.08% for the MLU, and the LSTM models show an MRE of 3.74–10.38% for the MLU. More importantly, both the training and forecasting errors of the above models are lower, in most cases, than those reported in the literature. Moreover, these results indicate that the transportation supply or the infrastructure-based accessibility (represented by logsum) significantly influences MLU patterns.

Keywords: logsum; accessibility; mixed land use; entropy index; machine learning; land parcel

check for updates

Citation: Almansoub, Y.; Zhong, M.; Safdar, M.; Raza, A.; Dahou, A.; Al-qaness, M.A.A. Modeling Impact of Transportation Infrastructure-Based Accessibility on the Development of Mixed Land Use Using Deep Neural Networks: Evidence from Jiang'an District, City of Wuhan, China. *Sustainability* **2023**, *15*, 15470. https://doi.org/10.3390/su152115470

Academic Editors: Dan Liu, Zhongyi Zuo and Zhongzhen Yang

Received: 6 October 2023
Revised: 24 October 2023
Accepted: 26 October 2023
Published: 31 October 2023

Copyright: © 2023 by the authors. Licensee MDPI, Basel, Switzerland. This article is an open access article distributed under the terms and conditions of the Creative Commons Attribution (CC BY) license (https://creativecommons.org/licenses/by/4.0/).

1. Introduction

The fast growth of urbanization, motorization, and technological innovations significantly alter human activities and the urban environment [1]. The classification of human activity by land use types, such as residential, commercial, and industrial, is a well-established practice in urban and transportation planning around the world. Classified land uses are segregated into distinct locations within cities based on rigorous zoning restrictions that consider the compatibility to avoid undesirable environmental problems resulting from the industrial revolution during the 19th and 20th centuries [2]. However, segregated land use was first criticized in 1960 by Jane Jacobs due to its numerous negative externalities, such as creating a sprawling urban area, increasing the use of private automobiles that scattered services and facilities, and safety issues [3]. In developed countries, land use policies and decision-making processes are generally more established and mature compared to those in developing countries like China. The differences can be attributed to various historical, economic, social, and political factors. For instance, the concept of the "compact city" has been widely promoted by urban planners in European countries [4]. The New Urbanism Congress' charter emphasizes the importance of compact, mixed neighborhoods. Through its core principles, it promotes the development of vibrant, diverse, and sustainable communities. Among these principles, one key aspect is the emphasis on compact and mixed-use neighborhoods [5]. Furthermore, the American Planning Association (APA) considers that MLU communities that are livable could be developed to promote efficient and sustainable land development and utilization, as well as to improve the diversity and energy of urban residents' lives [6]. Contrarily, urban and regional planning/modeling in China is not yet developed enough to effectively address the highly self-organized nature of MLU development, which is pervasive throughout the country. In most cases, mixed land use buildings in China allocate their initial floors for commercial and office purposes, while the upper floors are designated for residential activities [7]. Regarding the national policy on MLU in China, cities like Shanghai and Shenzhen have taken the lead in implementing appropriate policies to experiment with mixed land use developments. However, Beijing, the capital of China, has yet to issue relevant policy documents related to MLU [8].

A neural network (ANN) is a computational model that focuses on the structure and functions of ANN. DNN is one of several machine learning methods based on ANN [9]. The use of multiple layers in the network gives rise to the term 'deep' in DNN. DNN layers can also be heterogeneous and deviate significantly from biologically informed connectionist models. The primary purpose of these layers is to improve the model's efficiency. DNN applications have recently become a thriving field of study, with many practical applications and active research topics, such as in land use changes, including random forest [10], CNN [11], decision trees [12], and soft robotics modeling [13,14]. The results of using ANN revealed that temporal data frequently exhibit challenges, such as overfitting or nonlinear relationships, as well as redundancy dependence between multiple datasets [11]. DNN methods enable computers to learn from input data and comprehend the world through the use of a concept hierarchy [15]. Because of DNN's ability to learn a hierarchy of concepts, it was interesting to focus on how neural network functions affect land use changes over time, while incorporating temporal data of the transport supply. Land use change research has improved the semantic interoperability of the existing land use classification systems significantly [16]. Historically, studies on land use change have focused on matching conceptual definitions of land use types rather than the specific purpose of transportation supply. Although there has been significant progress in recent years in predicting the effect of transportation supply on land use change, the results are still not used often in DNN for predicting the effect of transportation supply on MLU. It can assist us in generating meaningful MLU changes for use in DNN. It can be applied to other areas of land use and transportation planning. As a result, the goal of this paper is to address this issue.

Gradually, traditional land use planning has incorporated mixed land use (MLU) as one of the most helpful and efficient methods to complement segregated land use

patterns. In the 1980s, urban planners urged the implementation of MLU due to its potential advantages. MLU has received attention in the 21st century as a mixed zoning scheme to provide facilities and services in a centralized location, and tends to encourage public transit, job generation, reduce the use of private cars, and CO_2 emissions [17,18]. Most of the existing studies utilize statistical methods to assess the relationship between travel distance and MLU at the aggregate level (e.g., at the zonal level) [8,19,20]. Only a few studies have employed cellular automata with machine learning to simulate MLU changes using remote sensing imagery data [10,11]. However, the literature shows that these studies have not fully examined the driving force of the MLU patterns. Furthermore, the influence of transport supply on MLU, particularly at the parcel level, has not been studied. Geographically, previous studies have mostly been undertaken in developed nations such as the United States [21,22], and the Netherlands [23,24], as well as few studies, being performed in developing nations such as India [25–27], Sri Lanka [12], South Korea [20], and China [10,11]. This study demonstrates conclusively that most methodologies are traditional, and that MLU types are treated as aggregate levels, which has been criticized in the literature due to the higher variability and failure to capture the MLU changes at the parcel level. In addition, there is a lack of exploration of more advanced DNN methods such as DNN and LSTM in this context.

Owing to the lack of a sound, scientific planning process in developing countries, there is a dire need to address these challenges efficiently. Segregated land use was criticized for numerous reasons such as soaring car ownership, urban sprawling, and mismanagement of allied facilities and services. However, the existing research results are limited in explaining the driving mechanism of transport supply on MLU patterns and the development of related forecasting models. To address these issues, this study is devoted to analyzing the impact of transport supply on MLU and developing related forecasting tools. This study utilizes real-world data to study the driving role of transport on MLU patterns, extract important factors affecting MLU patterns, and systematically study transport and MLU at the most disaggregate (parcel) level. In this study, MLU data at the parcel level are used to carry out the above research, offering a vivid portrayal of MLU dynamics. This approach ensures a precise representation of land development and significantly enhances the utility of the findings in policy analysis [28], when compared to the previous research implemented at zonal level. Through a comprehensive literature review of MLU studies, we have identified three main research questions that require further investigation in the realm of MLU research: (i) The impact of transportation infrastructure-based accessibility measures for MLU at the parcel level across different transportation modes. (ii) The lack of a modeling approach that delves into the mechanisms of both internal and external driving factors influencing MLU. (iii) The lack of a comprehensive method to effectively analyze and handle nonlinear complex data within the context of MLU research.

The objectives of this study are three-fold: first, the four-step modeling approach is adopted to calculate the logsum by different modes such as walk, bike, bus, subway, car, and taxi to the MLU parcel considered, which is used to represent the transport supply at the parcel level. Second, to fill the gap within the previous research, the current study uses the system dynamics theory to analyze the mechanism of internal and external driving factors of MLU, in order to understand the causal relationship between transport systems, and MLU patterns. Third, the state-of-the-art DNN techniques (e.g., MLP and LSTM), are used to develop quantitative models to quantify the effects of transport supply on MLU at the parcel level in Jiang'an District, Wuhan, China. In general, the results from this study should help to improve the scientific nature of urban land use and transport planning. The methods provided in this study may contribute to the more effective modeling/planning of urban areas. In addition, the methods may assist the government, stakeholders, and policymakers with a smart and inclusive sustainable urban development. Ultimately, precise, and comprehensive planning could have significant positive effects on public health, the country's economy, and sustainability.

The paper is structured into five sections. Section 2 reviews the relevant literature concerning transport supply and land use. Section 3, presents the study data and methodology. Section 4 presents the results and discussions. Finally, Section 5 summarizes the conclusions, limitations, and recommendations of this study.

2. Literature Review

In the early 21st century, mixed land use (MLU) emerged as a superior planning concept compared to segregated land use, leading to a notable shift in urban planning practices. Over the last two decades, there has been a clear and widespread adoption of MLU in modern city planning [29]. MLU development and transportation infrastructure-based accessibility are interdependent and interconnected. Well-planned transportation infrastructure facilitates the integration of diverse land use types, while MLU development increases transportation accessibility by reducing travel distances and promoting sustainable transportation alternatives. This symbiotic relationship contributes to the development of vibrant, connected, and sustainable communities [30,31]. For instance, Aygoren [32], suggests that if there are two primary uses, it should be classified as MLU. This definition is also adhered to by the Adelaide City Council, which defines vertical MLU developments as those that combine two or more land uses within a single vertical building. According to Hoppenbrouwer et al. [33], developers consider developments to be mix-use if planned, including three or more compatible uses, pedestrian scale, and public transport-oriented design. It allows compatible land uses to locate close to one another and thereby decreases the travel distances between activities. MLU indicates the diversity of functionally compatible land uses such as residential, commercial, industrial, institutional, and those related to transport [34] can be developed together, which offers many benefits. The application and recent advancement of DNN in various domains of artificial intelligence (AI) research. For instance, Maerten et al. [35] explores AI-generated art, examining DNN architectures and models used, from classic convolutional networks to cutting-edge diffusion models. In addition, Rodriguez-Conde et al. [36] presents a comprehensive overview of recent research that explores the convergence of artificial intelligence (AI) and the Internet of Things (IoT) within the framework of "smart everything". It focuses on designing mechanisms for collaborative inference across edge devices to execute complex DNN in resource-constrained infrastructures. Moreover, Lopez-Ballester et al. [37] explores the use of DNN approaches, specifically convolutional neural networks (CNNs), in estimating room acoustical parameters from speech signals in wireless acoustic sensor networks (WASNs). This advancement holds great promise for automatic monitoring systems in indoor environments, enabling efficient and accurate estimation of room acoustical parameters, without the need for specific impulse response measurements.

It is widely acknowledged that mixed-use neighborhoods tend to have urban form characteristics that may explain the lower levels of automobile dependence. Traditional neighborhoods are dense, mixed-use, and feature roadway networks organized in grids [20]. In addition, Choi et al. [9] used multiple regression to analyze regional data to address this issue. Independent variables included density and MLU. Partial correlations revealed that transit mode share was positively related to development density and MLU. Moreover, Munshi [27] examined the impact of accessibility on MLU using the GWR method. The results reveal that enhanced accessibility has led to an increase in mixed-use, high-density development along the transit line.

In the literature, a few statistical and artificial neural network (ANN) approaches have been employed to simulate and predict the MLU changes. The majority of the studies employed ANNs and cellular automata (CA) models [10,11,38], regression analysis [20], geographical regression analysis [8], and descriptive statistics [21], to simulate the MLU changes. In addition, few studies used machine learning techniques such as random forest [10], CNN [11], and decision trees [12] to simulate MLU changes. In the context of the MLU type, numerous studies have been tested at the aggregate levels (district, zone, block) [19,39,40], while a limited number of studies have been carried out at the

disaggregate levels to simulate MLU changes (parcel or grid cell) [22]. Geographically, most of the previous studies have been undertaken in developed nations such as the United States [21,22], and the Netherlands [23,24], as well as few studies, being performed in developing nations such as India [12,13], Sri Lanka [12], South Korea [20], and China [10,11]. This review demonstrates conclusively that most of the methodologies used in these previous studies are traditional, and that the MLU types are treated as aggregate levels, which has been criticized in the literature due to the higher variability and failure to capture the MLU changes at the parcel level.

To study the relationship between transport supply and MLU, this study employs state-of-the-art methods such as DNN (MLP and LSTM) models to examine the impact of transportation infrastructure-based accessibility on the prevalence of MLU patterns at the parcel level. DNNs have been regarded as a reliable method for displaying MLU changes [30,41]. The LSTM can extract information from sequential data sets [16,42,43]. DNNs are multi-layered extensions of traditional ANNs. DNN algorithms have gained popularity recently because of their exceptional capacity to process nonlinear data [11,15]. It is anticipated that these models will perform better than traditional regression models and statistical models. Second, the current study intends to study the effect of transport supply on MLU patterns at the parcel level, which has not been fully studied. Studying the driving force of the MLU pattern at the parcel level may provide practical planning tools and policies for encouraging MLU development. In this study, the entropy (ENT) and Herfindahl–Hirschman (HH) indexes are used to represent the MLU pattern [44].

Lastly, this study selects Jiangan District in the city of Wuhan, China to evaluate the relationship between transport supply and MLU. This study will provide precise forecasting and its findings may contribute to the development of a socially, economically, and environmentally sustainable city. In recent years, technological advancement has revolutionized the city's morphology, and city governments need to continuously adopt smart policies and solutions. This study could aid in designing the city efficiently and effectively through supporting policy formulation related to MLU development.

3. Study Data and Methods

3.1. Dataset

This study focuses on the case study of Jiang'an District in Wuhan, China. The city of Wuhan has 13 districts under its jurisdiction. Table 1 shows that the population of Jiang'an District in 2012 was 921,700 persons, and in 2015, it increased to 954,300 persons. In 2012 and 2015, there were 141 and 196 bus lines, respectively. There was only one subway line with 12 and 14 subway stations in 2012 and 2015, respectively. In recent years, the rapid development of the subway system in the city of Wuhan has accelerated, and between 2012 and 2015, the total length of completed subway lines increased dramatically, from 28.68 km to 125 km [19]. Furthermore, subway line 1 is the only subway line covering the study area which was constructed in 2004 and was then extended in 2010 and 2014 [19].

Table 1. Jiang'an District category study data.

Years	Bus Lines	Subway Stations	Population (Persons)	Parcels (Nos)
2012	141	12	921,700	871
2015	196	14	954,300	

The built floor space is categorized into six categories (residential, commercial, industrial, office, education, and other types such as services, etc.). Due to the data limitations, only four types of space categories are considered in this study: residential, mixed residential–commercial, commercial, and mixed commercial–residential.

Table 2 shows the average space price by space type and total space quantity. Figure 1a–c accordingly illustrate the Jiang'an District, Wuhan, and presents the area of the parcels

being studied, TAZ, and district, considered for this study, which was 22,276, 12,501,182, and 669,719,876 (Sqr Meter), respectively.

Table 2. Average floor space price (Yuan/m^2) and total space quantity (m^2).

Years/Type	2012		2015	
	Total Space Quantity	**Average Floor Space Price**	**Total Space Quantity**	**Average Floor Space Price**
Commercial	1,804,696	18,934	2,179,442	22,853
Mix (Commercial–Residential)	1,888,940	16,791	2,013,994	20,579
Residential	13,559,658	8027	14,804,345	10,749
Mix (Residential–Commercial)	19,163,936	9704	19,615,624	12,649
Total Space Quantity	36,417,230	-	38,613,405	-

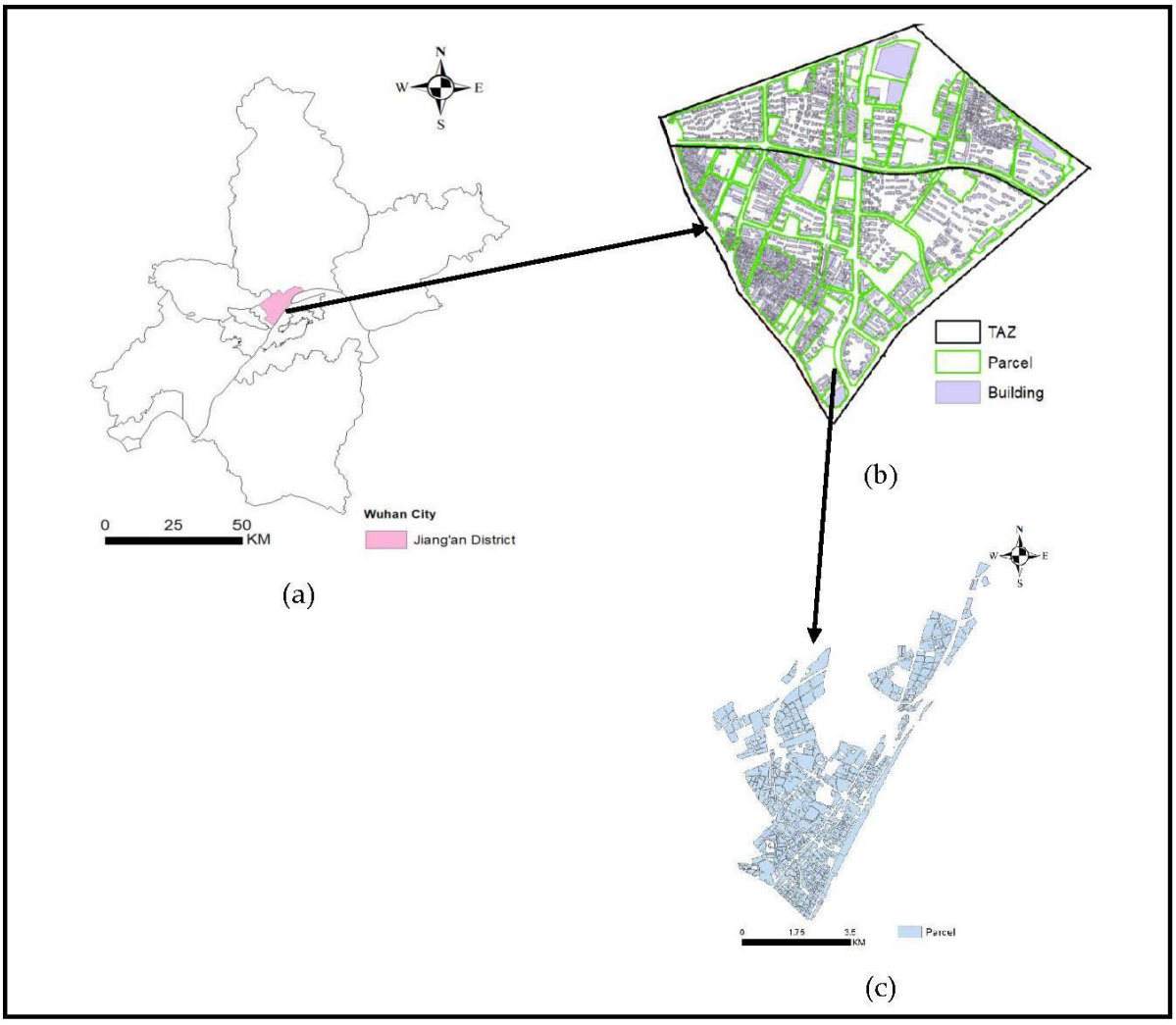


Figure 1. Several levels of paper dataset at the parcel level of the Jiang'an district: (**a**) Jiang'an District, Wuhan, (**b**) area of parcel, TAZ, and the district, (**c**) Jiang'an District parcels.

Figure 2a,b demonstrate the building data, and Figure 2c illustrates the changes in the building data from 2012 to 2015. The building data was used to develop the MLU patterns at the parcel level, which contains the building type and floor space quantity. In addition, the ArcGIS version 10.8 spatial intersection analysis tool and building data are used to calculate the floor space at each parcel. However, due to data limitations, this study only considers a horizontal mix, where we assume that each building is only for one type of use.

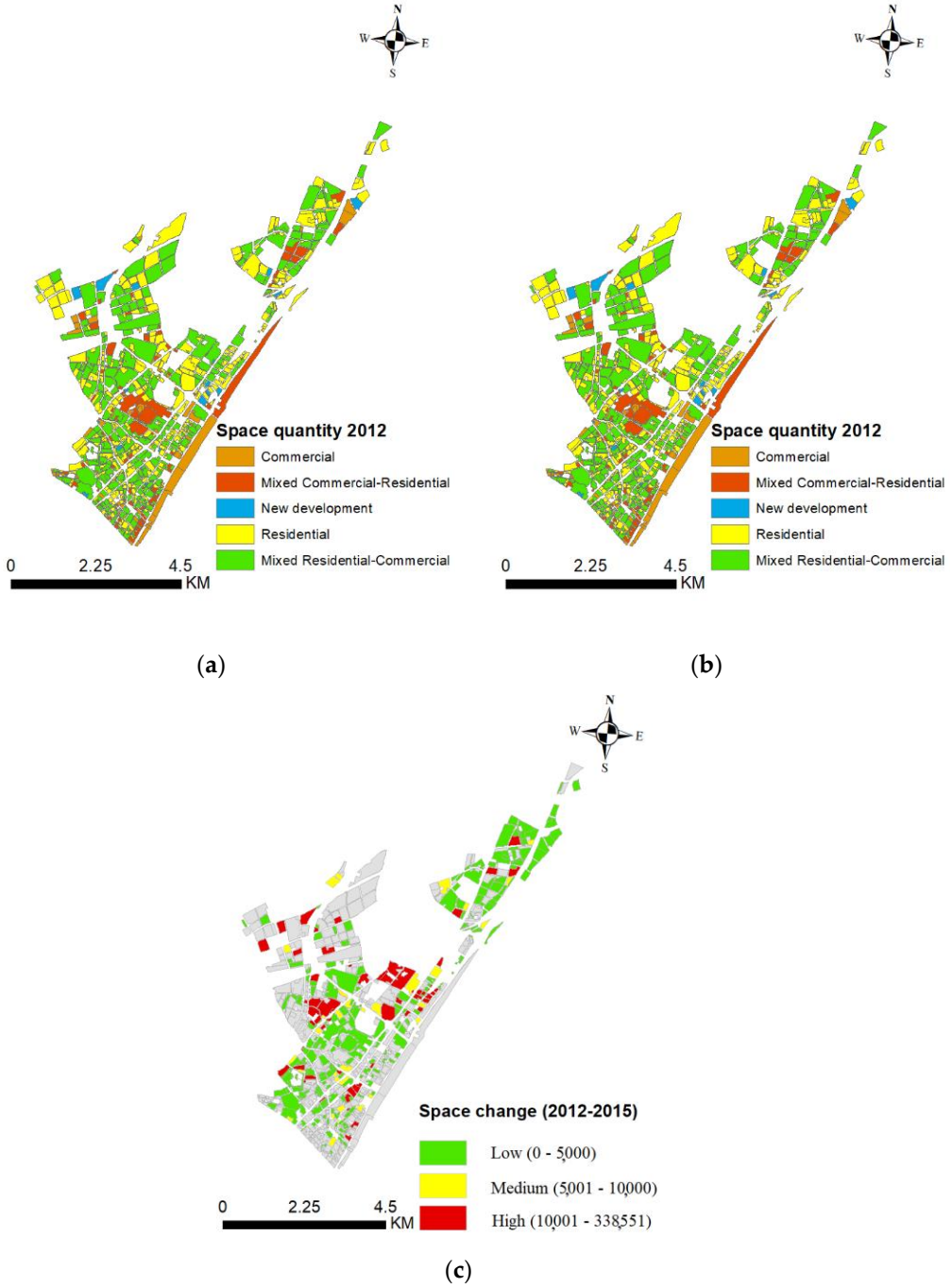


Figure 2. Building datasets of 2012 and 2015: (**a**) parcels by building type (2012), (**b**) parcels by building type (2015), (**c**) space changed from the years 2012 to 2015.

Subway line 1 was the first subway line, which started to operate in 2004. In 2012, subway line 1 had a total of 12 stations in the Jiang'an District. Subway line 2 is the second line operating in the city of Wuhan, with 21 stops. Subway line 4 is the third line of service. The first phase of the project was put into operation in 2013. Since Wuhan subway line 4 was only put into operation in 2013, there were 28 stations for the subway line 4 in 2015. Figure 3a,b show the number of subway stations and subway line 1 in the study area in 2012 and 2015, respectively.

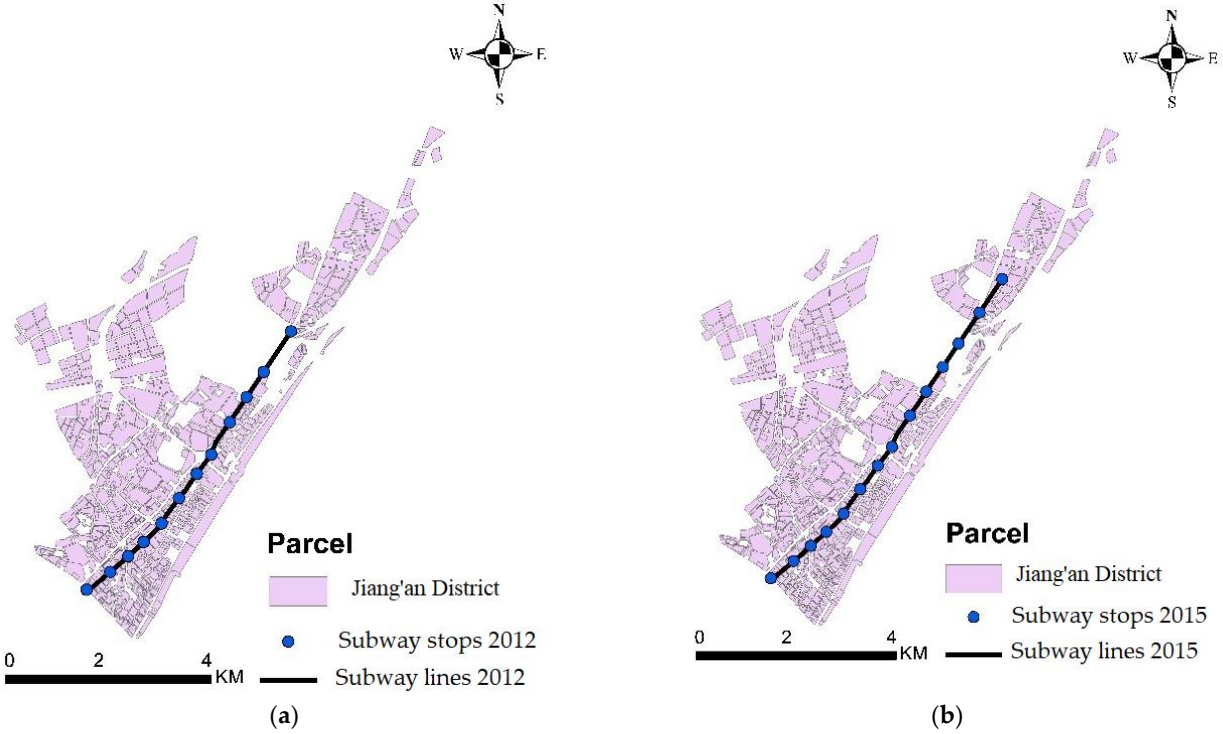


Figure 3. Subway line 1 and subway stations in Jiang'an District: (**a**) subway line 1 and subway stations (2012), (**b**) subway line 1 and subway stations (2015).

3.2. Floor Space Price Process

Figures 4a–c and 5 show the floor space prices in the Jiang'an District, which were obtained using the ArcGIS Kriging interpolation tool. Table 3 shows the number of parcels with a certain type of land use type and the corresponding floor space price available in Jiang'an district, for example, the number of residential locations was 72 and 90, and their average price was 8150 and 9901 (Yuan/m^2) in 2012 and 2015, respectively. However, the number of commercial locations were 20 and 30, and their average prices were 18,640 and 19,294 (Yuan/m^2) in 2012 and 2015, respectively. To calculate the prices for the rest of the study areas, the kriging interpolation method was used. This method converts the study areas into raster grid cells. Furthermore, the raster grid cell was converted to point features using a tool called the "raster to point", then, the parcels layer and the point data of the average floor space price were spatially linked.

Table 3. Observed space prices (Yuan/m^2) before kriging interpolation.

Land Use Type	2012		2015	
	Number of Locations	Average Price	Number of Locations	Average Price
Residential prices	72	8150	90	9901
Commercial prices	20	18,640	30	19,294

Figure 6a–d show the average floor space price between 2012 and 2015, as calculated using kriging interpolation. Furthermore, in Figure 6a, a range of indexes is used to represent the residential space price in 2012 as the following: the low space price (5683~6502), low-medium space price (6503~7370), medium space price (7371~8520), medium-high space price (8521~10,070), and high space price (10,071~12,015). Moreover, Figure 6b displays the average residential floor space price calculated in 2015 using kriging interpolation. The range of indexes used to represent space prices, from high to low, are as follows: high space price (14,673~17,633), medium-high space price (12,473~14,672), medium space price (10,563~12,472), low-medium space price (8936~10,562), and low space price (7673~8935).

Figure 6c illustrates the commercial prices in 2012 with the index values falling within the ranges of high space price (21,227~22,518), medium-high space price (18,989~21,226), medium space price (16,615~18,988), low-medium space price (14,884~16,614), and low space price (12,928~14,883). Additionally, Figure 6d depicts the commercial prices in 2015, with index values ranging from high space price (23,293~27,675) to low space price (13,612~15,392). These index ranges offer a detailed representation of the space and commercial prices in the given context.

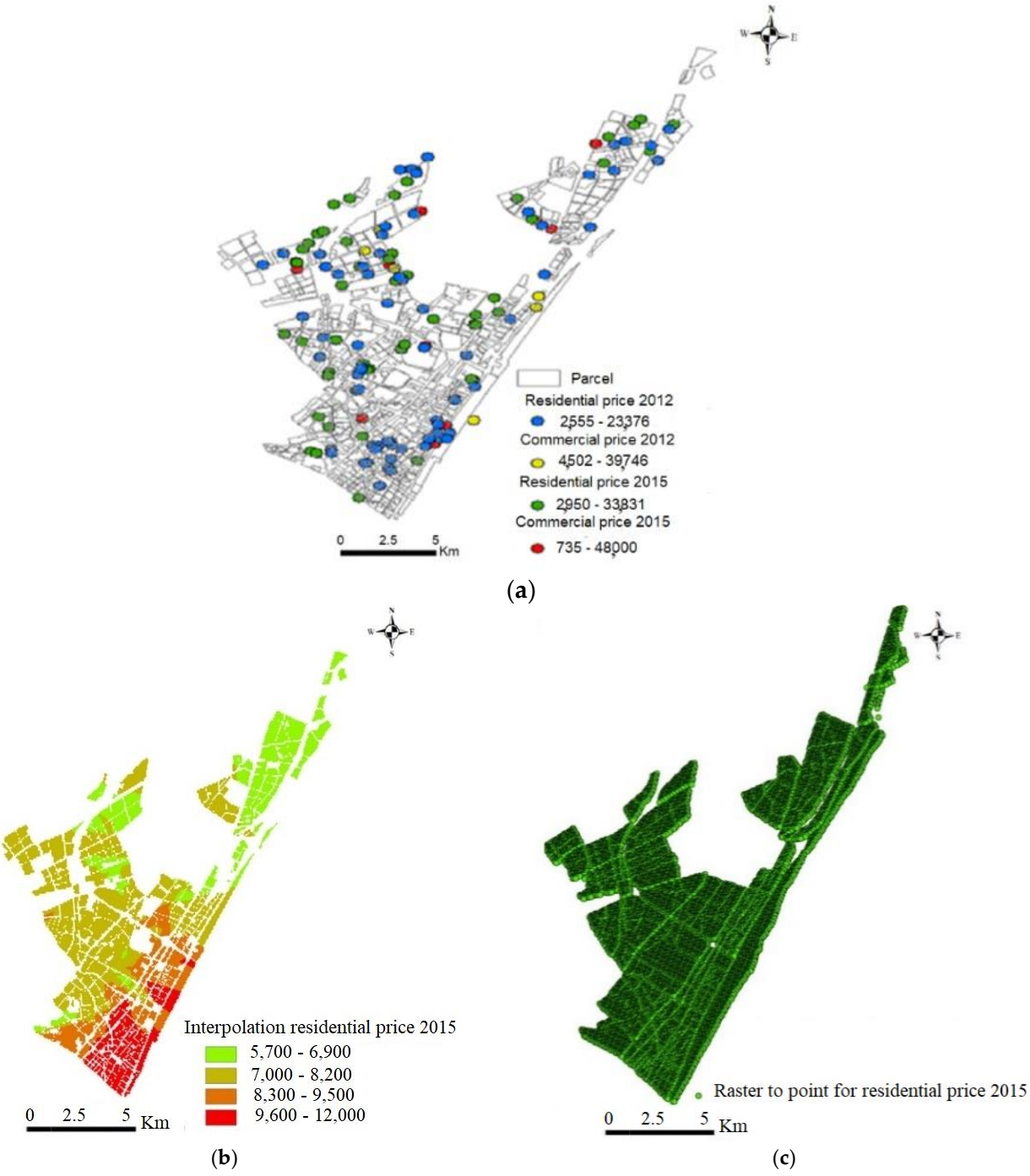


Figure 4. Interpolated residential prices:(**a**) land use prices before kriging interpolation, (**b**) kriging interpolation as a raster, (**c**) raster to points conversion.

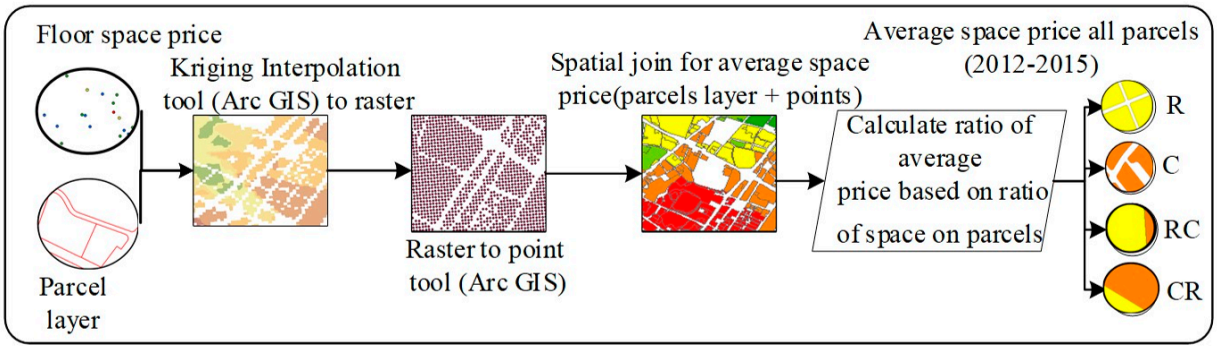


Figure 5. Floor space price estimation using kriging interpolation (Yuan/m^2).

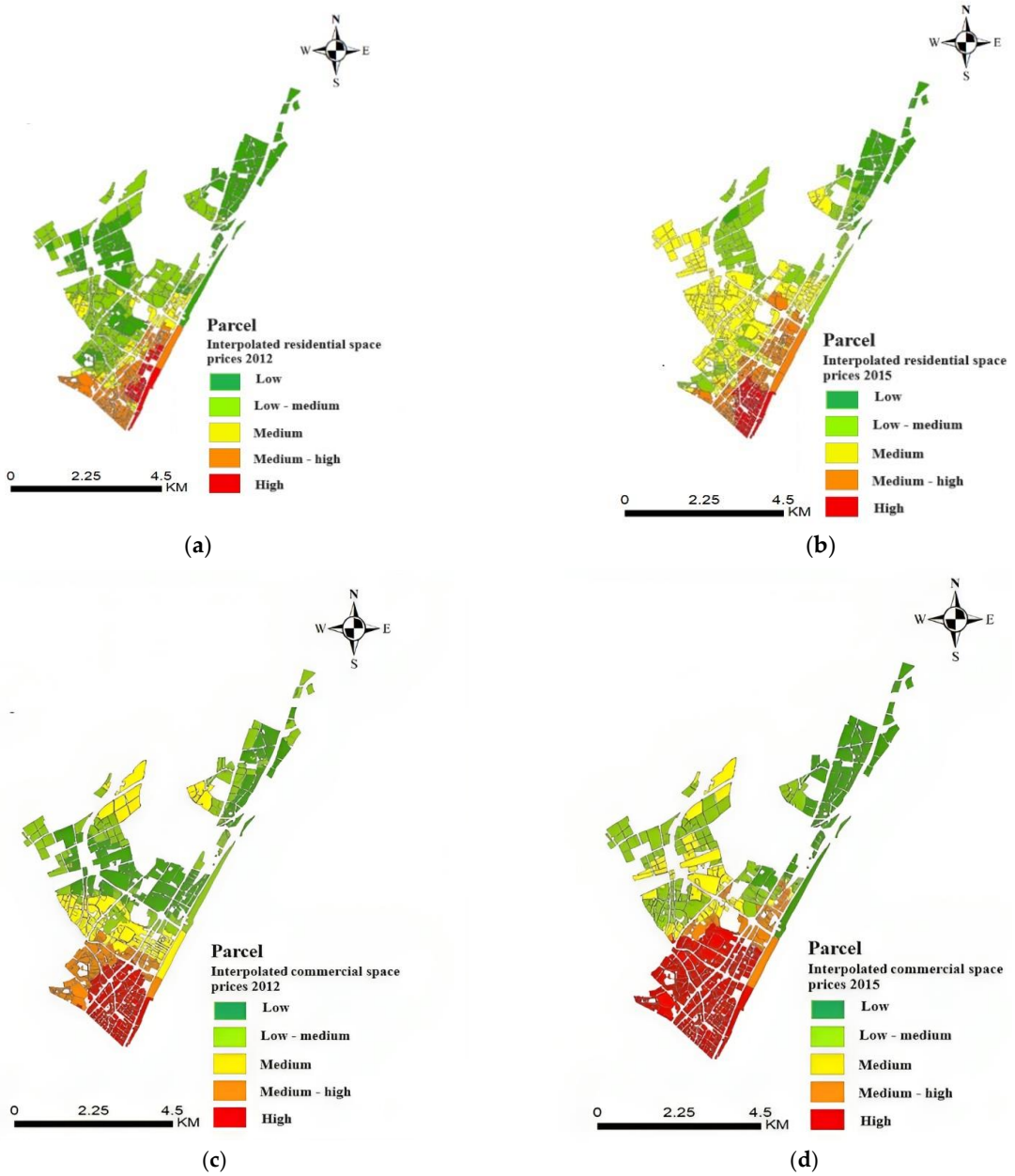


Figure 6. Residential and commercial floor space prices for 2012 and 2015; (**a**) residential average price in 2012; (**b**) residential average price in 2015; (**c**) commercial average price in 2012; and (**d**) commercial average price in 2015.

3.3. Methods

DNNs are enhanced versions of traditional ANNs. ANNs are a reliable method for performing increasingly complex calculations on a set of inputs to address problems in the real world. Therefore, in this study, the impact of transport supply on MLU is examined using DNNs, such as MLP and LSTM. Figure 7 illustrates the proposed workflow. The following are the main steps:

(1) Prepare data for models that represent transport supply (subway lines and stops, bus stops and lines, road network), average floor price, and MLU pattern (building and developable land);
(2) The developed multimodal transportation model is used to estimate the logsum by walk, bike, bus, subway, car, and taxi;
(3) The average floor space prices are calculated utilizing the kriging interpolation tool;
(4) The spatial join and intersection analysis tool in ArcGIS is utilized to prepare the MLU pattern data at the parcel level. Then, the ENT and HH indexes are employed to represent the degree of MLU;
(5) Utilize the system dynamic framework to examine the causal relationship between transport supply, various other related factors, and MLU;
(6) DNNs (MLP and LSTM) are utilized to forecast the influence of transport supply on MLU;
(7) Finally, compare the accuracy of the LSTM and MLP.

3.3.1. Analysis of the Causal Relationship between MLU and Transportation Supply Using a System Dynamics Diagram

System dynamics have been extensively used in integrated land use transport studies. The feedback and connections provided by these models are useful for defining the interactions among variables within an urban system [45]. The causal loop diagram (CLD) is a useful tool for identifying potential sources of dissent to strategies, repercussions within the system, and synergies. These prospects aid in the identification of potential problem statements that can be addressed through quantitative modeling. A CLD depicts the interrelationships among important variables using text, arrows, and symbols. A polarized arrow extending from "cause" to "effect" represents the interaction between two variables, also known as a causal connection. In the CLD, the "+" sign on the arrow line indicates that a factor is positively correlated with another [46]. The system dynamics model is then validated by collecting data to prove the relationship between various influencing factors and MLU.

In this study, we used multiple regression analysis to examine the relationship between the dependent variable (e.g., quantity of MLU, space demand, multimodal transportation demand) and the independent variables such as the supply of multimodal transportation, space price, space supply, population density, employment density, road network, bus stations, and routes, rail transit stations and routes, available land, and floor area ratio within the SD diagram. The mathematical form of multiple regression used in the SD diagram is presented in Equation (1):

$$Y = a + \sum_{i=1}^{n} b_i \times x_i \quad (1)$$

where

— Y represents the dependent variable;
— a represents the constant or intercept;
— b_i represents the estimated regression coefficient slope of the y regression on the independent variable Xn;
— x_i represents the independent variable or factors such as space price, space supply, population, employment, road network, bus stations and routes, and rail transit stations and routes, available land, and floor area ratio.

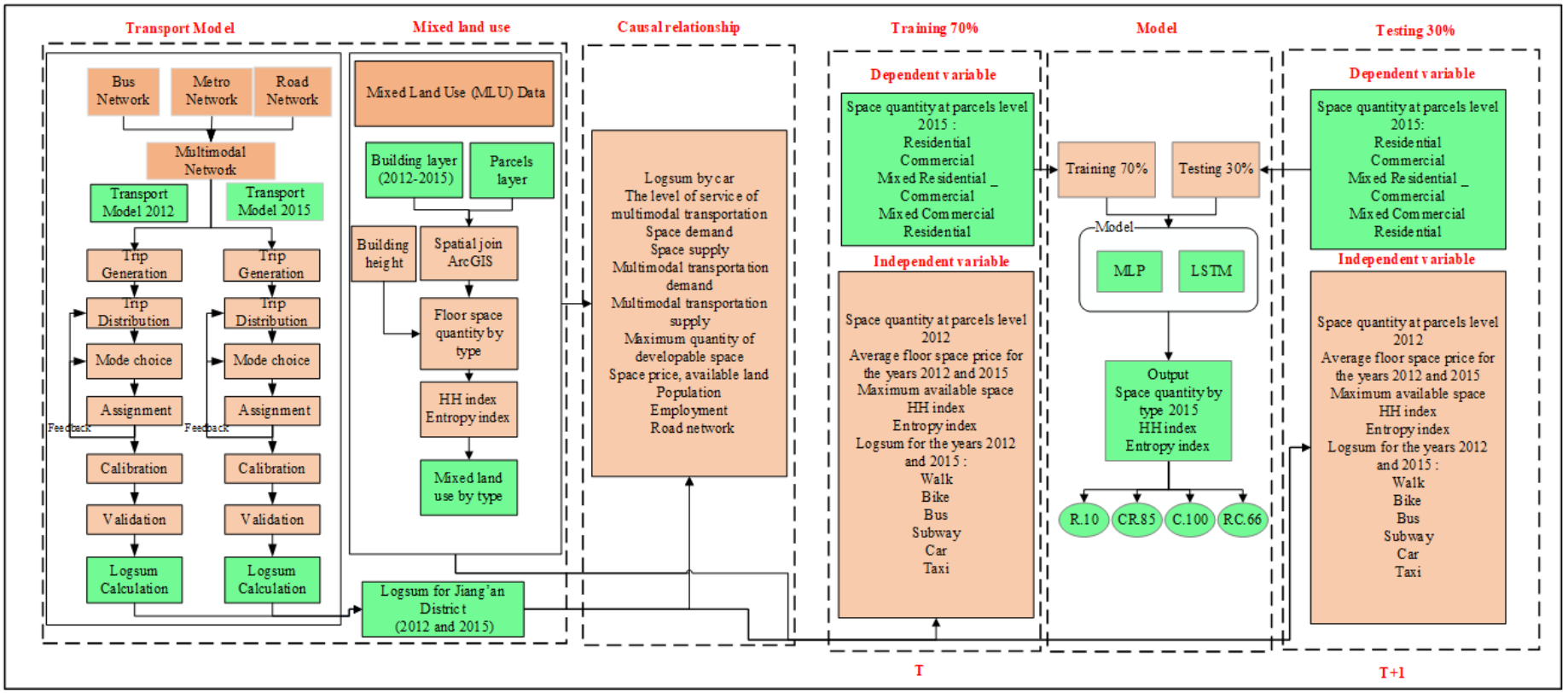


Figure 7. The workflow of the proposed modeling process.

3.3.2. Parameters for Representing/Modeling MLU Patterns

MLU presents diverse land use into an area, making it a crucial tool for spatial planning. The MLU model was developed utilizing the building data, as shown in Figure 8. The parcel data include the number of floors of a building(s), building area, and type of building as shown in Figure 9a,b. Spatial analysis was used to extract the parcel data using ArcGIS intersection tools. Additionally, to estimate the built space quantity by parcel type, the extracted parcel area and the number of floors were utilized.

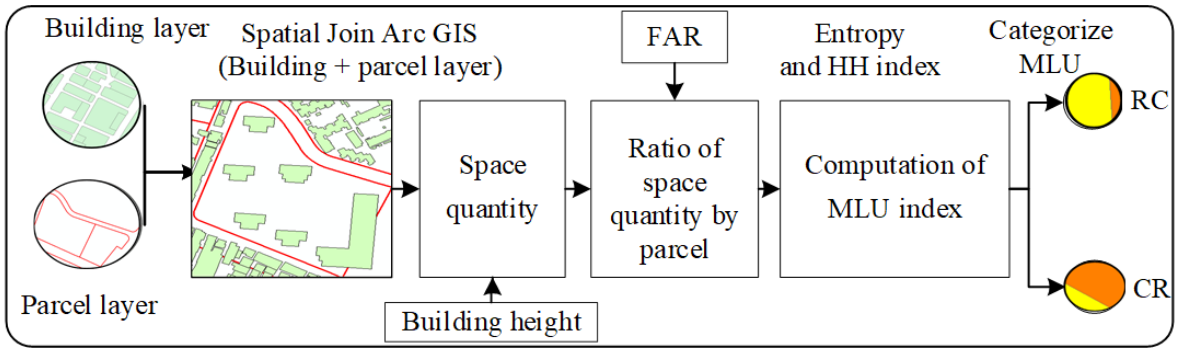
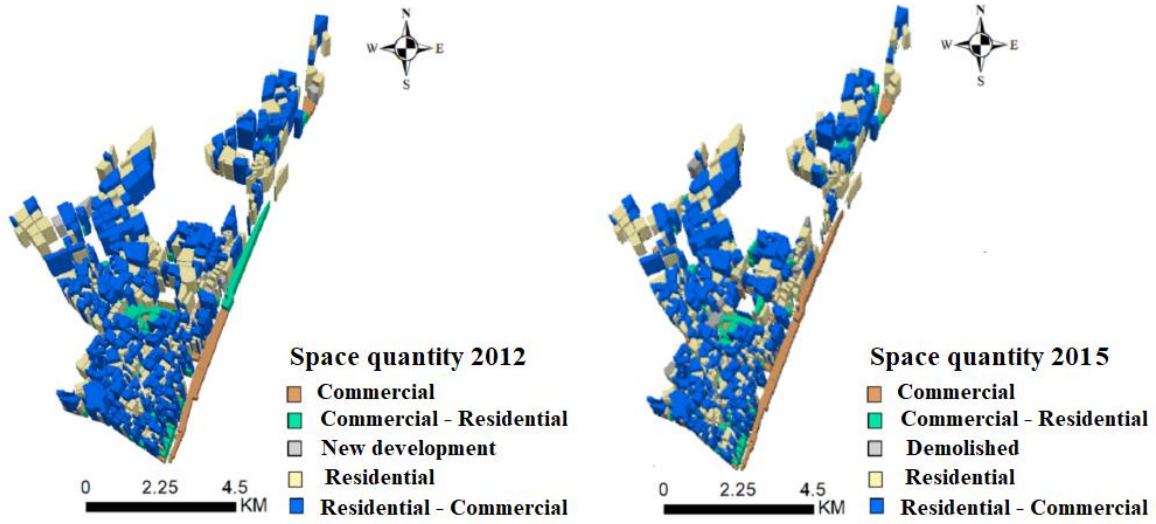


Figure 8. The procedure for preparing data.



(**a**) (**b**)

Figure 9. Building data types; (**a**) building data type 2012; (**b**) building data type 2015.

The floor area ratio (FAR) is used to represent the density of the developed MLU pattern, which is the ratio between the built floor space and the land of the parcel being developed, and it is shown in Equation (2). One of the city policies requires a collection of the total building data in order to identify the FAR for every parcel (Jayasinghe et al. [12]).

$$FAR = \frac{\sum_{j=1}^{n} B_i \times F_i}{A} \quad (2)$$

where

- FAR is the maximum floor area ratio;
- B_i is the total floor area (m^2) of the building i;
- F_i is the number of floors of the i the building;
- A is the area of the parcels under calculation.

Equation (3) is used to calculate the maximum available space quantity with the maximum floor area percentage and developable land use (3).

$$MaxQ_i^p = AL_i^p \times FAR^p \tag{3}$$

where

- $MaxQ_i^p$ is the maximum developable space;
- p is the land use in the parcels i;
- AL_i^p is the developable land of the parcel;
- FAR^p is the maximum floor area ratio.

The data was analyzed using two different MLU indexes: ENT and HH indexes. The ENT index measures the different types of land use in an area, with a higher entropy degree representing a higher level of MLU [47,48]. A higher HH index indicates a lower level of MLU. To calculate the MLU diversity, the ENT index was used. The ENT index ranges from 0 to 1. If the value is 0, there is no MLU pattern, whereas 1 indicates a high degree of MLU. The HH index ranges from 0 to 100 in this study. If the value is 100, there is no MLU pattern, whereas 0 indicates a high degree of MLU. The ENT index measurement of a specific area of land use diversity is estimated by Equation (4). The HH index is used in economics to measure the market concentration and is related to the level of MLU [44]. The HH index is estimated utilizing Equation (5) as follows:

$$ENT = -(\sum_{j=1}^{k} P^j ln P^j)/ln(k) \tag{4}$$

where

- P^j represents the ratio of each type of land use;
- k represents the aggregate number of different types of land use in parcels j.

$$HHI = \sum_{j=1}^{k} (100 \times P^j)^2 \tag{5}$$

where

- P^j represents the ratio of different types of land use within a parcel;
- k represents the total number of different types of land use within a given parcel.

3.3.3. Transport Model

The transportation model is proposed to estimate the logsum for the years 2012 and 2015. To depict the interactions between all modes of transport, this model was developed utilizing a multimodal network model. As outlined in Section 3.1, diverse datasets were utilized, and a series of steps were executed to calculate the logsums at the parcel level. These logsums served as independent variables in both MLP and LSTM models. The modeling process involved the following steps:

(1) The trip generation module begins by estimating trip production and attraction rates using population, employment, and household data;
(2) The trip distribution approach uses the gravity model to distribute these trips to every parcel;
(3) A mode choice module: Transport utilities are calculated based on trip purposes (e.g., home-based work, home-based other, home-based school, and non-home-based) and transportation modes (including, bus, metro, bike, taxi, and personal car). These calculations are then incorporated into the nested logit model, as outlined in Table 4. The parameter β's value fluctuates based on the trip purpose and the presence of a personal car. In this study, we specifically focus on trips related to home-based work and home-based other, both of which involve personal car usage. The attribute coefficients for various transportation modes, including in-vehicle time β1, waiting

time β2, walking time β3, subway and bus fare β4, transfer time β5, β6, and cost per km by different trip purposes (HBW, HBO, HBS, and NHB), were obtained from the Wuhan Transportation Planning Institute (WHTPI) for different trip purposes (HBW, HBO, HBS, and NHB) (source: http://www.whtpi.com/Default.html, accessed on 15 April 2022).

Table 4. Transport utilities by trip purpose and by modes.

	Home-Based Work (HBW) Car Available						**Home-Based Other (HBO) Car Available**					
Modes	β1	β2	β3	β4	β5	β6	β1	β2	β3	β4	β5	β6
Metro	−0.02	−0.04	−0.04	−0.039	−0.1	−0.2	−0.02	−0.04	−0.04	−0.078	−0.1	−0.2
Bus	−0.02	−0.04	−0.04	−0.039	−0.2		−0.02	−0.04	−0.04	−0.078	−0.2	
Taxi	−0.02	−0.04	−0.039				−0.02	−0.04	−0.078			
Car	−0.02	−0.04	−0.039				−0.02	−0.04	−0.078			
Bike	−0.02	−0.04					−0.02	−0.04				
	Home-based school (HBS)						**Non-home-based (NHB)**					
Modes	β1	β2	β3	β4	β5	β6	β1	β2	β3	β4	β5	β6
Metro	−0.02	−0.04	−0.04	−0.305	−0.1	−0.2	−0.02	−0.04	−0.04	−0.114	−0.1	−0.2
Bus	−0.02	−0.04	−0.04	−0.305	−0.2		−0.02	−0.04	−0.04	−0.114	−0.2	
Taxi	−0.02	−0.04	−0.305				−0.02	−0.04	−0.114			
Car	−0.02	−0.04	−0.305				−0.02	−0.04	−0.114			
Bike	−0.02	−0.04					−0.02	−0.04				

Equations (6)–(10) outline the determination of an individual's preferences for specific transport modes tailored to particular trip purposes. In this study, we consider the motorized modes such as personal car (U_car), subway ($U_{_subway}$), bus (U_bus), and taxi ($U_{_taxi}$), walk ($U_{_walk}$), and bike ($U_{_bike}$). Figure 10 depicts the structure of the nested logit model.

$$U_{Metro} = \beta1 \times T_{IV} + \beta2 \times T_{IW} + \beta3 \times T_W + \beta4 \times F_M + \beta5 \times T_{MMT} + \beta6 \times T_{MBT} \quad (6)$$

$$U_{Bus} = \beta1 \times T_{IV} + \beta2 \times T_{IW} + \beta3 \times T_W + \beta4 \times F_B + \beta5 \times T_{TT} \quad (7)$$

$$U_{Taxi} = \beta1 \times TIV + \beta2 \times TW + \beta3 \times CD \quad (8)$$

$$U_{Car} = \beta1 \times T_{IV} + \beta2 \times T_W + \beta3 \times C_D \quad (9)$$

$$U_{Bike} = \beta1 \times T_{IV} + \beta2 \times T_W \quad (10)$$

where the following are defined:

- T_{IV} = In-Vehicle Time (actual time spent in the vehicle);
- T_{IW} = Initial Waiting Time at transit stations;
- T_W = Walking Time from home to transit stations, and waiting time in the case of a taxi; access time in the case of a car and bike;
- F_M = Metro Fare;
- T_{MMT} = Metro-to-Metro Transfer Time;
- T_{MBT} = Metro-to-Bus Transfer Time;
- F_B = Bus Fare;
- T_{TT} = Bus-to-Bus and Bus-to-Metro Transfer Time;
- C_D = Cost per Kilometer for driving a car.

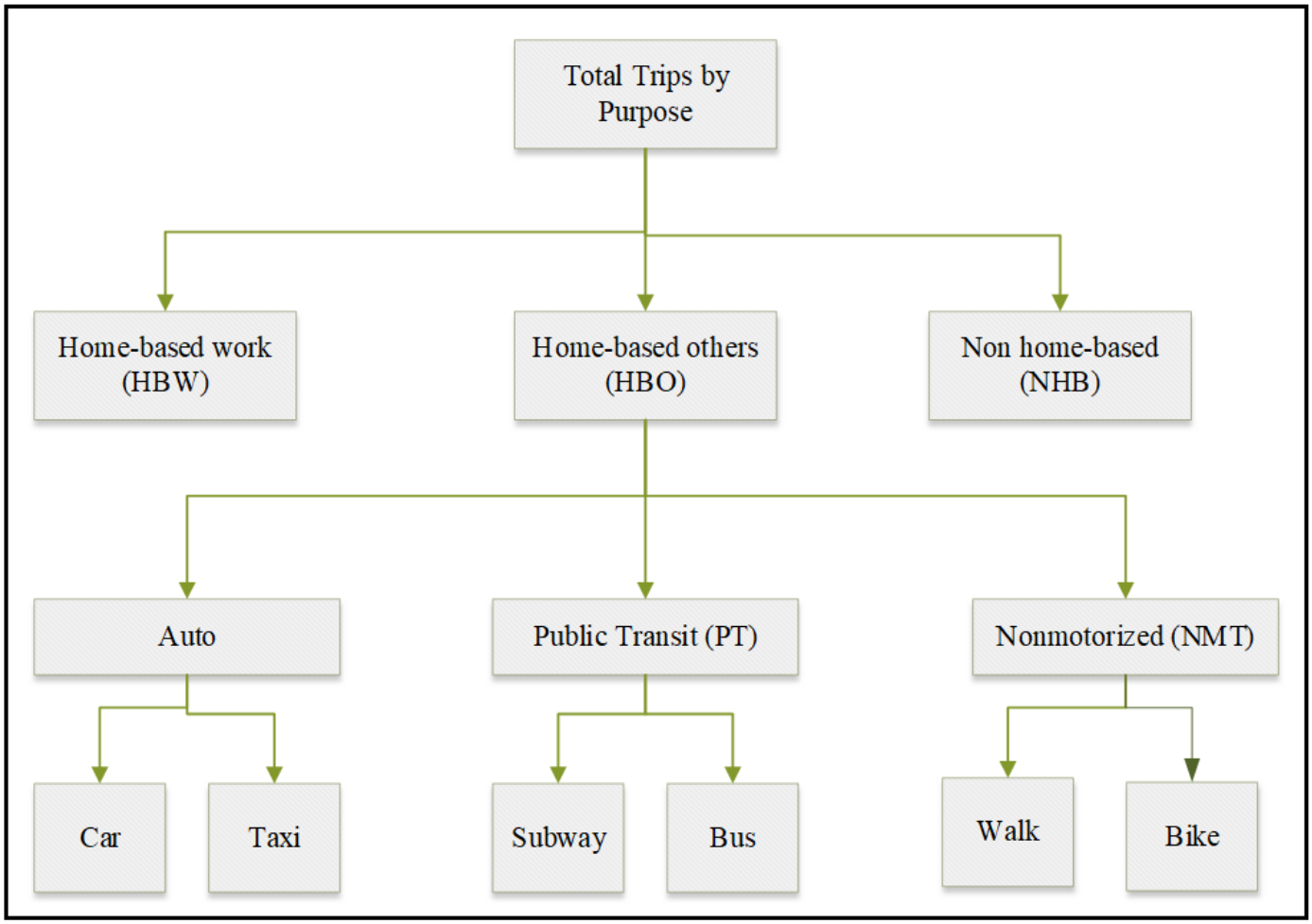


Figure 10. Nested logit model structure.

The mode choice module uses the congested travel time, transport utilities, and scaling parameters to allocate trips to various modes. These parameters have been both calculated and calibrated to match the observed mode preferences for different mode types.

(4) The network assignment (user-equilibrium) and transit assignment (multi-routing) were developed to calculate congested travel time by all modes.
(5) Furthermore, these measures are used to calculate the logsum of various modes (such as bike, bus, subway, car, and taxi), as shown in Equation (11).
(6) Lastly, these data are utilized as independent variables in the MLP and LSTM approaches.

$$A_i = \mathrm{Ln} \sum_{j=1}^{n} \sum_{k=1}^{m} e^{U_{ij}^k} \tag{11}$$

where

- A_i represents the logsum of parcel i;
- i and j together represent the number of parcel;
- k represents one of the transport modes;
- n represents the total number of parcels;
- m represents the total number of transport modes;
- U_{ij}^k represents the utility produced by the transport mode k between parcel i and j.

In addition, the above equation used for calculating the logsum for different parcels which can be accessed by different transport modes such as (walk, bike, bus, subway, car,

and taxi). The transportation model was developed to estimate the logsum for the years 2012 and 2015, as shown in Figure 11.

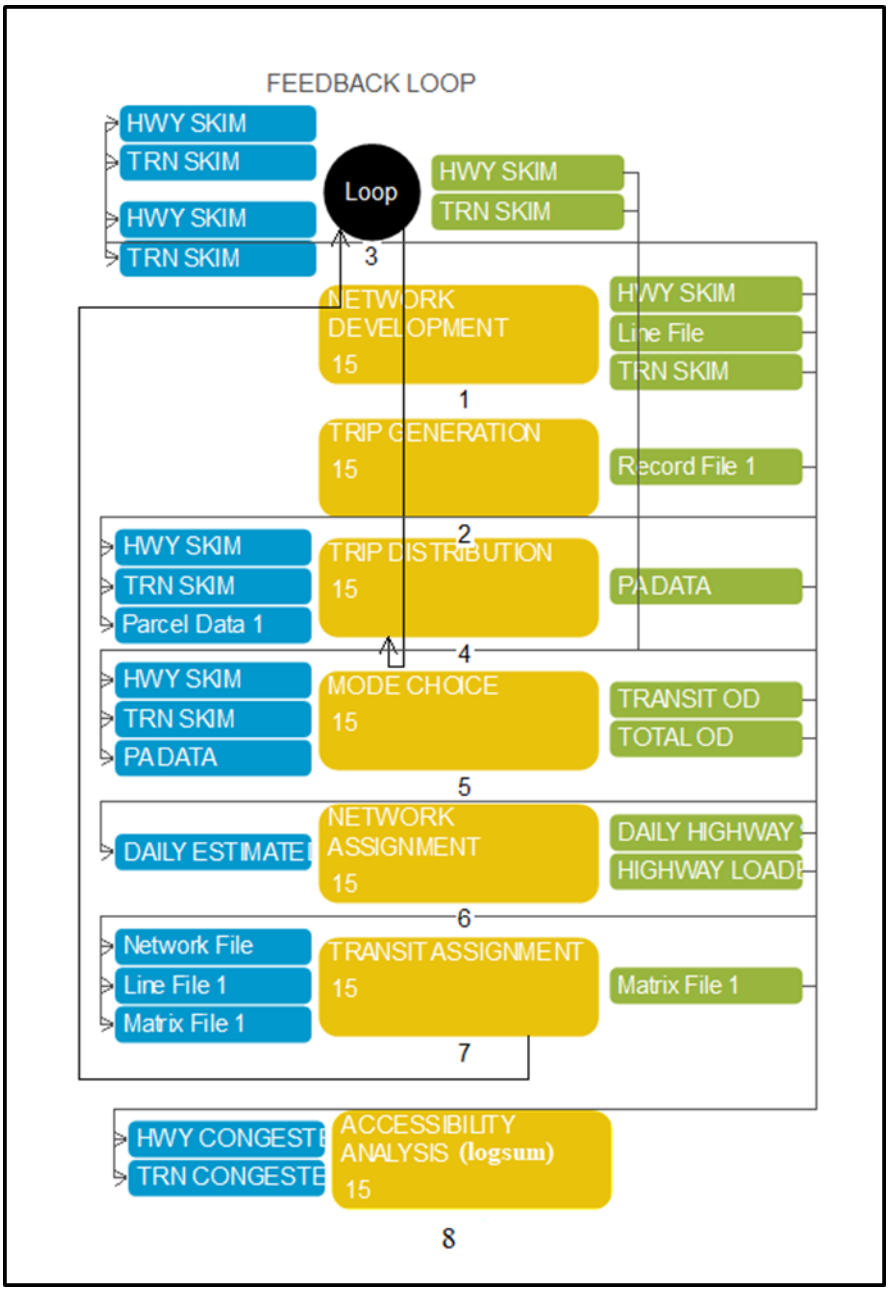


Figure 11. Transport model development framework.

3.3.4. Multilayer Perceptron (MLP) Model

DNNs are enhanced iterations of conventional multi-layer ANNs. DNN models are becoming more and more popular recently because of their better capacity to handle non-linear data. However, recent studies indicate that ANN-based methods have a significant potential for modeling MLU changes [9]. The impact of transport supply on MLU changes was examined using the ANN methods. In the corresponding layer, the unidirectional interconnections between neurons are represented by lines, while neurons are represented by circles [9]. Figure 12 depicts the MLP structure.

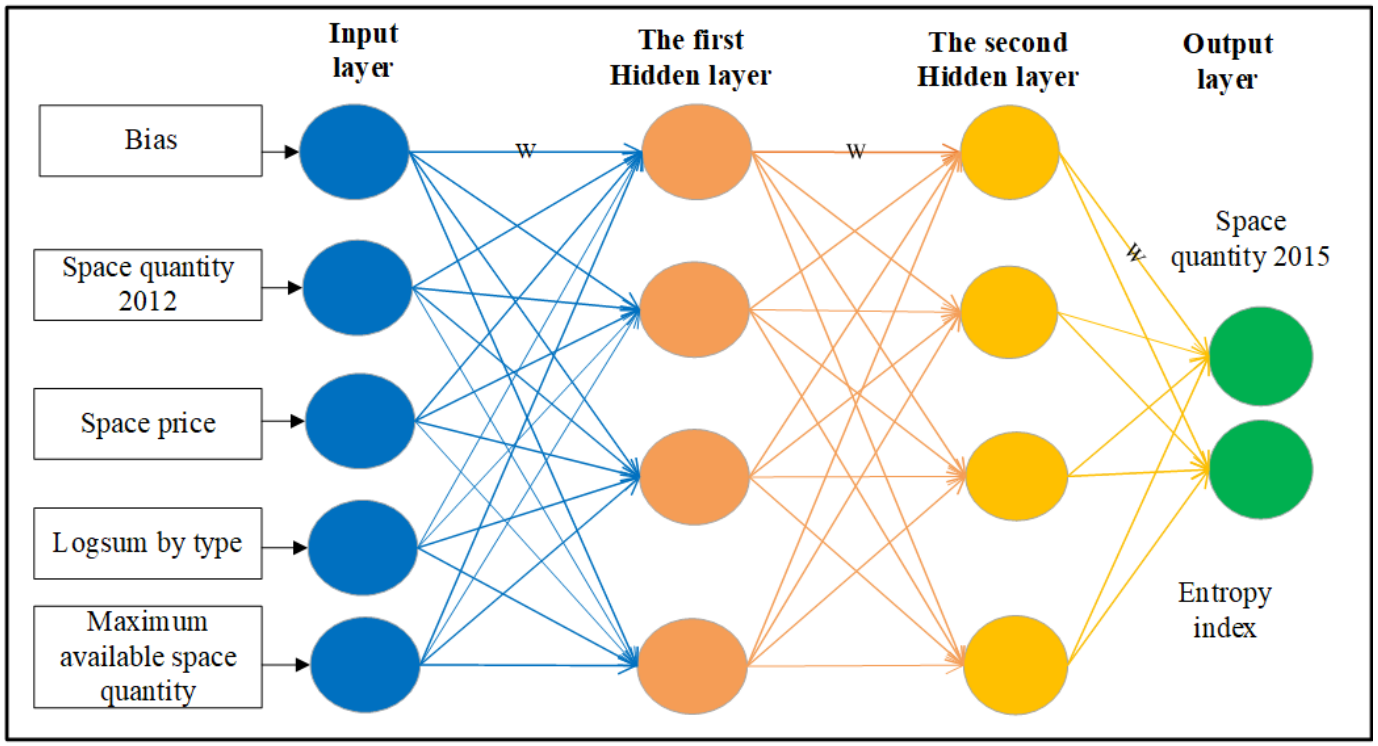


Figure 12. Architecture of MLP neural networks.

The input takes 13 variables: average floor space price, various logsum (by walk, bike, bus, subway, car, and taxi), space quantity, and maximum quantity of developable space. The output is the forecast space quantity in 2015. The mathematical equation of the MLP is shown in Equations (12) and (13).

$$Z_i = \sum_{i=1}^{m} w_{ij} \times x_i + b_j \tag{12}$$

$$Output\ Y_i = \mathrm{F}(Z_i) = \begin{cases} 1\ if \sum_{i=1}^{m} w_{ij} \times x_i + b_j \geq 0 \\ 0\ if \sum_{i=1}^{m} w_{ij} \times x_i + b_j < 0 \end{cases} \tag{13}$$

where

- Z_i represents the neuron's output value j;
- m represents the number of neurons in the previous layer;
- x_i represents the neuron's i input value in space quantity for the year 2012, average floor price, logsum, etc;
- w_{ij} represents the weight;
- b_j represents the bias;
- Y_i represents the output following neuron j activation (the forecast of space quantity for 2015);
- F represents the activation function.

The mean squared error used to calculate the loss function between each element in the input x and target y.

The unreduced (i.e., with reduction set to 'none') loss is defined as

$$L(X.Y) = \mathrm{L} = \{\{L_1 \ldots L_N\}^T\}.L_n = (X_n - y_n)^2 \tag{14}$$

in which N refers to the batch size, whereas if the reduction is not 'none' (default 'mean'), then

$$L(X.Y) = \begin{cases} \text{mean (L). if reducation = mean;} \\ \text{sum (L). if reducation = sum;} \end{cases} \quad (15)$$

where

- X and Y represent the tensors of arbitrary shapes with a total of n elements each;
- The mean operation still operates over all the elements, and divides by N;
- The division by N can be avoided if one sets reduction = 'sum'.

Finally, mean relative errors (MREs) were used to estimate the errors, the mathematical equation of the MRE is shown in Equation (16).

$$MRE = \frac{1}{N}\sum_{i-1}^{N}\left|\frac{P_i - O_i}{O_i}\right| \times 100\% \quad (16)$$

where

- MRE represents mean relative error;
- N represents the total number of parcels i;
- P_i represents the predicted value;
- O_i represents the observed value.

3.3.5. Long Short-Term Memory (LSTM) Model

The LSTM model, a subtype of recurrent neural networks (RNNs), is developed to overcome the vanishing gradient problem [49]. LSTMs are more commonly used than traditional RNNs due to their larger memory capacity. The LSTM incorporates components such as the cell state, input gate, forget gate, output gate, sigmoid activation, and *tanh* activation [50]. The input and output variables designed for the LSTM model are the same as the MLP model: the training set takes 70% of all the sample data and the testing set takes the remaining 30%. In Section 3.3.4., Equations (17)–(22) depict the RNN process, and Figure 13 depicts the architecture of the LSTM neural networks. The structure of the LSTM model can be formulated as follows:

$$i_t = \sigma(w_i[h_{t-1}, x_t] + b_i) \quad (17)$$

$$f_t = \sigma(w_f[h_{t-1}, x_t] + b_f) \quad (18)$$

$$\mathrm{o_t} = \sigma(\mathrm{w_o}[\mathrm{h_{t-1}}, \mathrm{x_t}] + \mathrm{b_o}) \quad (19)$$

$$\mathrm{g_t} = tan\ h\left(\mathrm{w_g}[\mathrm{h_{t-1}}, \mathrm{x_t}] + \mathrm{b_g}\right) \quad (20)$$

$$c_t = f_t \times c_{t-1} + i_t \times g_t \quad (21)$$

$$h_t = o_t \times tan\ h(c_t) \quad (22)$$

where:

- $\mathrm{i_t}$ represents the input gate, and $\mathrm{g_t}$ indicates cell activation;
- $\mathrm{f_t}$ denotes forget gate;
- $\mathrm{o_t}$ denotes the output gate, where σ refers to the sigmoid function;
- w denotes the weight, b indicates bias;
- $\mathrm{c_t}$ represents cell state, and $\mathrm{h_t}$ is the hidden state.

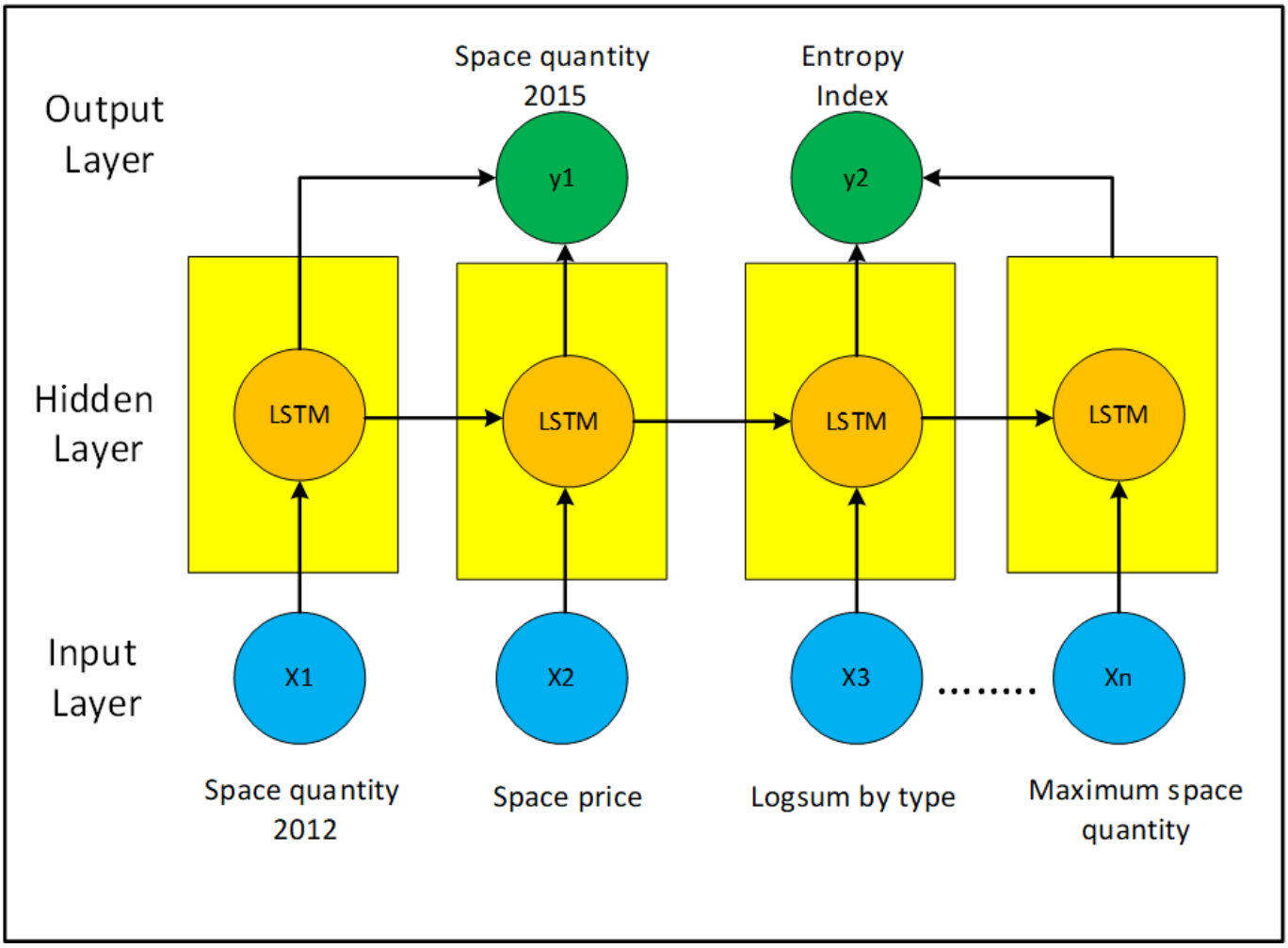


Figure 13. LSTM neural network structure.

4. Results and Discussion

DNN (MLP and LSTM) approaches are utilized to study the effect of transport supply, which is represented by a logsum, onto the level of MLU at the parcel level.

4.1. Results of the Causal Relationship between Transport Supply and MLU

This study employs a system dynamic approach to examine the relationship between various indicators, including transport supply, and MLU [51]. In particular, A CLD is used to analyze various factors that have a causal relationship with the MLU, such as housing price, population, employment, and transportation supply as shown in Figure 14 [52]. Based on the concept of representative variables and the knowledge regarding their relationship, Figure 14 is developed, which shows that an increase in the logsum of the multimodal transportation system to the city center, retail, and services will result in a rise in the floor space prices [53]. Furthermore, due to the limited land available for development, the rising floor space prices may lead to an increase in MLU developments to accommodate the growth of the population and employment [54]. Because of the increase in employment and the population, the road network and other public facilities must be expanded [55].

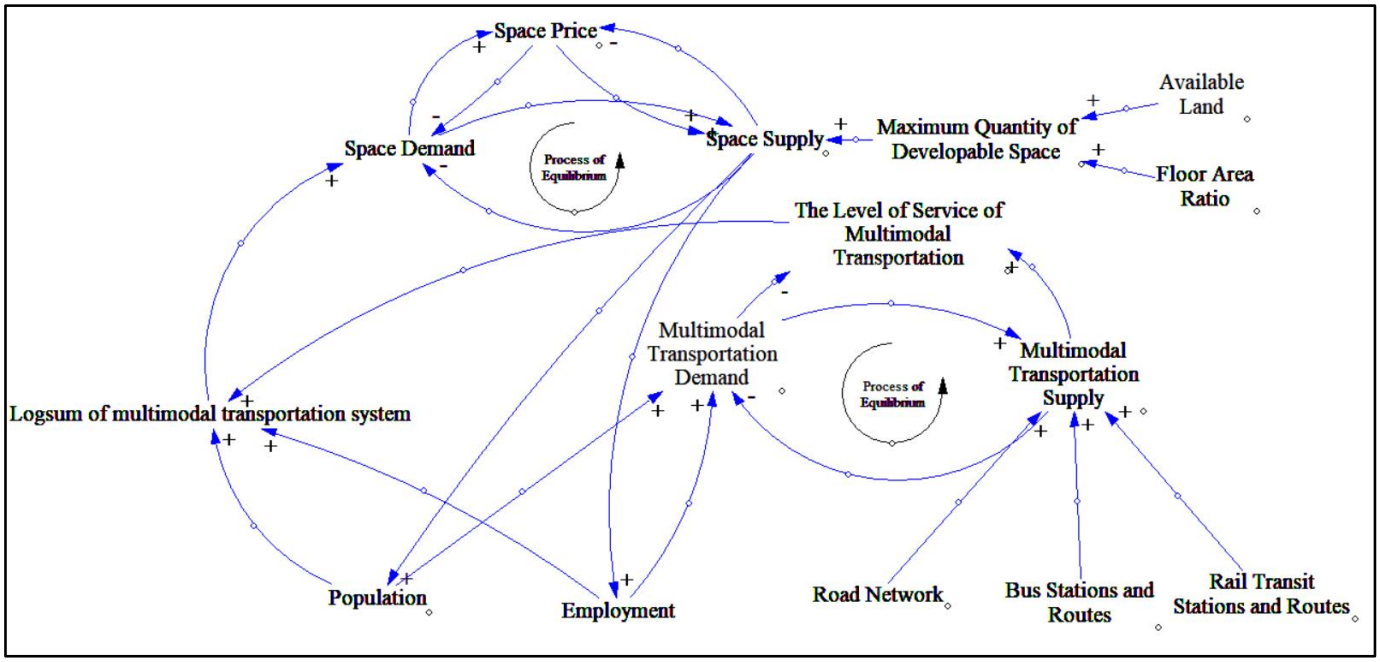


Figure 14. A causal relationship between various factors and MLU using a system dynamic framework.

In system dynamics theory, horizontal variables are used to represent the state of the system at different times. These variables do not change quickly under the accumulation of time, but they are affected by the input and output flow rates. The input and output are defined as decision-making or rate variables in system dynamics theory, and the rate variables change with respect to the changes of the level variables and decision variables. Specifically, the level variable transmits the received information to the rate variable, and the change in the rate variable produces a corresponding change in the level variable.

The mathematical relationship between variables such as the logsum of the multimodal transportation system (MTS), the level of service of multimodal transportation (LSMT), space demand (SD), space supply (SS), multimodal transportation demand (MTD), multimodal transportation supply (MTS), maximum quantity of developable space (MQS), space price (P), available land (AL), population (PP), employment (E), and road network (RN) are proposed and they are shown in Equations (23)–(27):

$$Logsum = a_1 * PP + a_2 * E + a_3 * LSMT \quad (23)$$

$$SD = a_4 * P + a_5 * SS + a_6 * logsum \quad (24)$$

$$MTD = a_7 * PP + a_8 * E + a_9 * MTS \quad (25)$$

$$MTS = a_{10} * RN + a_{11} * B + a_{12} * RT \quad (26)$$

$$MQS = a_{13} * AL + a_{14} * FAR \quad (27)$$

where

- *Logsum* represents the logsum of multimodal transportation system (MTS);
- *PP* represents the population density;
- *E* represents the employment density;
- *LSMT* represents the level of service of multimodal transportation;
- *P* represents the space price;
- *SD* represents the space demand;
- *SS* represents the space supply;

- MTD represents the multimodal transportation demand;
- MTS represents the multimodal transportation supply;
- RN represents the road network;
- B represents the number of bus stations and routes;
- RT represents the number of rail transit routes and stations;
- MQS represents the maximum quantity of developable space;
- AL represents the available land;
- FAR represents the floor area ratio;
- $a_1.a_2 \ldots a_{14}$ are the coefficients of the variables.

Table 5 shows the degrees of correlation between variables. Using 2015 as an example, different space quantity types are identified: (CR = commercial–residential, RC = residential–commercial, C = commercial, R = residential). In Table 5, the majority of variables have probability values (p-values) between 1% and 5%, indicating a strong correlation with the space quantity. The outcomes indicated that the logsum by subway is highly correlated with residential space in the year 2015 and with mixed commercial–residential space in 2012. Moreover, Table 5 shows that transport supply (represented by the logsum) significantly influences space prices.

In this study, multiple regression analysis is used to examine the relationship between the dependent variables and independent variables. It is also used to diagnose the multi collinearity of the variables. The model's goodness-of-fit and accuracy are evaluated using the coefficient of determination (R^2) and mean absolute percent error (MAPE) metrics. The results of the multiple regression analysis are presented in Tables 6 and 7, which show that the developed models, including the logsum by multimodal transportation, space demand, multimodal transportation demand, multimodal transportation supply, and maximum quantity of developable space, had acceptable levels of accuracy. The R^2 values for these models are 0.66, 0.75, 0.62, 0.72, and 0.68, respectively, with a level of significance of 0.00, indicating a satisfactory level of accuracy. The study concludes that the developed models are suitable for modeling dependent variables such as the logsum by MTS, space demand, multimodal transportation demand, multimodal transportation supply, and the maximum quantity of developable space in a given area based on many factors including space price, space supply, population, employment, road network, bus stations and routes, rail transit stations and routes, available land, and floor area ratio for the years 2012 and 2015.

4.2. Logsum and MLU Change at the Parcel Level for the Years 2012 and 2015

This paper uses six categories of logsum measures, including the logsum by walk, bike, bus, subway, car, and taxi in the study area (Jiang'an District), during the years 2012 and 2015.

4.2.1. Logsum by Walk

Figure 15a,b depict the logsum by walk at the parcel level for the years 2012 and 2015. The findings showed that most areas with a high logsum by walk are associated with a higher density of mixed (RC and CR) space quantities being developed. Due to the increase in the logsum by walk in 2015, a considerable increase in the mixed space quantity was discovered for the parcels located in the center and south of Jiang'an District, near the subway line 1 and the city center. These findings suggest that there is a strong relationship between "the logsum by walk" and mixed space quantity. Figure 15a,b illustrate the spectrum of index values for the logsum by walk in 2012 and 2015: the lowest logsum between (0.00~3.56) in the north of Jiang'an District, medium (3.57~3.96) in the center and north of Jiang'an District, medium-high (3.97~4.16) in the center of Jiang'an District, and the highest (4.17~4.32) in the south of Jiang'an District.

Table 5. Correlation matrix.

No	Pearson Correlation	(1)	(2)	(3)	(4)	(5)	(6)	(7)	(8)	(9)	(10)	(11)	(12)	(13)	(14)	(15)
(1)	Commercial Space (CS) 2012	1														
(2)	Commercial–Residential Space (CRS) 2012	−0.050	1													
(3)	Residential Space (RS) 2012	−0.063 *	−0.082 **	1												
(4)	Residential–Commercial Space (RCS) 2012	−0.074 *	−0.096 **	−0.122 **	1											
(5)	Commercial Space (CS) 2015	0.835 **	−0.042	−0.063 *	−0.074 *	1										
(6)	Commercial–Residential Space (CRS) 2015	−0.042	0.924 **	−0.084 **	−0.092 **	−0.051	1									
(7)	Residential Space (RS) 2015	−0.063 *	−0.082 **	.914 **	−0.107 **	−0.063 *	−0.084 **	1								
(8)	Residential–Commercial Space (RCS) 2015	−0.075 *	−0.090 **	−0.103 **	0.965 **	−0.075 *	−0.100 **	−0.124 **	1							
(9)	Logsum Walk 2015	0.044	0.051	−0.046	−0.015	0.041	0.053	−0.046	−0.014	1						
(10)	Logsum Bik 2015	0.027	0.031	−0.001	−0.011	0.025	0.032	0.001	−0.010	0.939 **	1					
(11)	Logsum Bus 2015	0.038	0.049	−0.026	−0.018	0.034	0.048	−0.012	−0.016	0.712 **	0.667 **	1				
(12)	Logsum Subway 2015	0.008	0.058 *	−0.077 *	−0.069 *	−0.008	0.051	−0.095 **	−0.078 *	0.499 **	0.537 **	0.247 **	1			
(13)	Max Available Space	−0.045	−0.062 *	0.260 **	0.437 **	−0.051	−0.067 *	0.280 **	0.447 **	−0.034	0.082 **	−0.040	−0.167 **	1		
(14)	Residential Price 2015 (RP)	0.004	0.172 **	−0.185 *	−0.170 *	0.003	0.041	−0.112 *	−0.247 **	0.168 **	0.156 **	0.178 **	0.074 *	−0.463 **	1	
(15)	Commercial Price 2015 (CP)	0.130	0.052	−0.106 *	−0.219 **	0.031	0.051	0.023	0.040	0.108 **	0.058 *	0.335 **	0.335 **	−0.285 **	0.748 **	1

Note: * Correlation is significant at the 0.05 level (2-tailed), ** Correlation is significant at the 0.01 level (2-tailed). R = residential, C = commercial, RC = residential–commercial, CR = commercial–residential.

Table 6. Model summary by multiple regression analysis.

Model	Dependent Variables	R Square	Adjusted R Square	Std. Error of the Estimate
1	Logsum by MTS	0.66	0.65	1.26
2	Space Demand	0.75	0.75	0.59
3	Multimodal Transportation Demand	0.62	0.60	1.15
4	Multimodal Transportation Supply	0.72	0.70	0.96
5	Maximum Quantity of Developable Space	0.68	0.66	1.03

Table 7. Coefficients by multiple regression analysis.

	Dependent Variables	Independent Variables	Unstandardized Coefficients		Standardized Coefficients	t-Values	Significance (*p*-Values)
			B	Beta	Beta		
1	Logsum by MTS	Population	1.36	0.09	0.78	14.98	0.00
		Employment	1.17	0.03	0.82	38.73	0.00
		The Level of Service of Multimodal Transportation	0.85	0.10	0.49	8.41	0.00
		Space Price	0.94	0.11	0.54	8.96	0.00
2	Space Demand	Space Supply	4.70	0.77	0.37	6.11	0.00
		Logsum by car	3.81	0.75	0.30	5.10	0.00
3	Multimodal Transportation Demand	Population	0.93	0.03	0.65	13.14	0.00
		Employment	0.31	0.07	0.23	30.55	0.00
		Multimodal Transportation Supply	1.86	0.47	0.36	3.98	0.00
4	Multimodal Transportation Supply	Road Network	3.81	0.75	0.30	5.10	0.00
		Bus Stations and Routes	4.00	0.38	0.24	10.46	0.00
		Rail Transit Stations and Routes	0.80	0.03	0.56	23.91	0.00
5	Maximum Quantity of Developable Space	Available Land	0.31	0.07	0.23	4.55	0.00
		Floor Area Ratio	3.81	0.75	0.30	5.10	0.00

4.2.2. Logsum by Bike

Figure 16a,b depict the logsum by bike at the parcel level for the years 2012 and 2015. The findings reveal that areas with a high logsum by bike indicate a high density of mixed (RC and CR) space quantity being developed. Due to the increase in the logsum by bike in 2015, a considerable increase in the mixed space quantity was observed for the parcels located in the center and south of Jiang'an District, close to subway line 1 and the city center. These findings suggest that there be a strong relationship between the logsum by bike and the quantity of mixed spaces. Figure 16a,b illustrate the index value range of "logsum by bike" in 2012 and 2015: the lowest logsum values are between (0.00~5.31) in the north of Jiang'an District, medium (5.32~5.45) in the center and north of Jiang'an District, medium-high (5.46~5.53) in the center of Jiang'an District, and the highest logsum (5.54~5.59) in the south of Jiang'an District.

4.2.3. Logsum by Bus

Figure 17a,b depict the logsum by bus at the parcel level for the years 2012 and 2015. The findings show that most areas with a high logsum by bus indicated a high density of mixed (RC and CR) space quantity being developed. Due to the increase in the logsum by bus in 2015, a considerable increase in the mixed space quantity was observed for the parcels located in the center of Jiang'an, District and a significant increase in mixed space quantity are found. The results reveal a robust association between the logsum values by bus and the quantity of mixed spaces. Figure 17a,b show the index value range of the logsum by bus in 2012 and 2015: the lowest logsum between (0.00~4.54) is found in the north and east of Jiang'an District, medium logsum (4.55~4.70) in the east of Jiang'an

District, medium-high logsum (4.71~4.87) in the center of Jiang'an District, and the highest logsum (4.88~5.06) is found in the center and south of Jiang'an District.

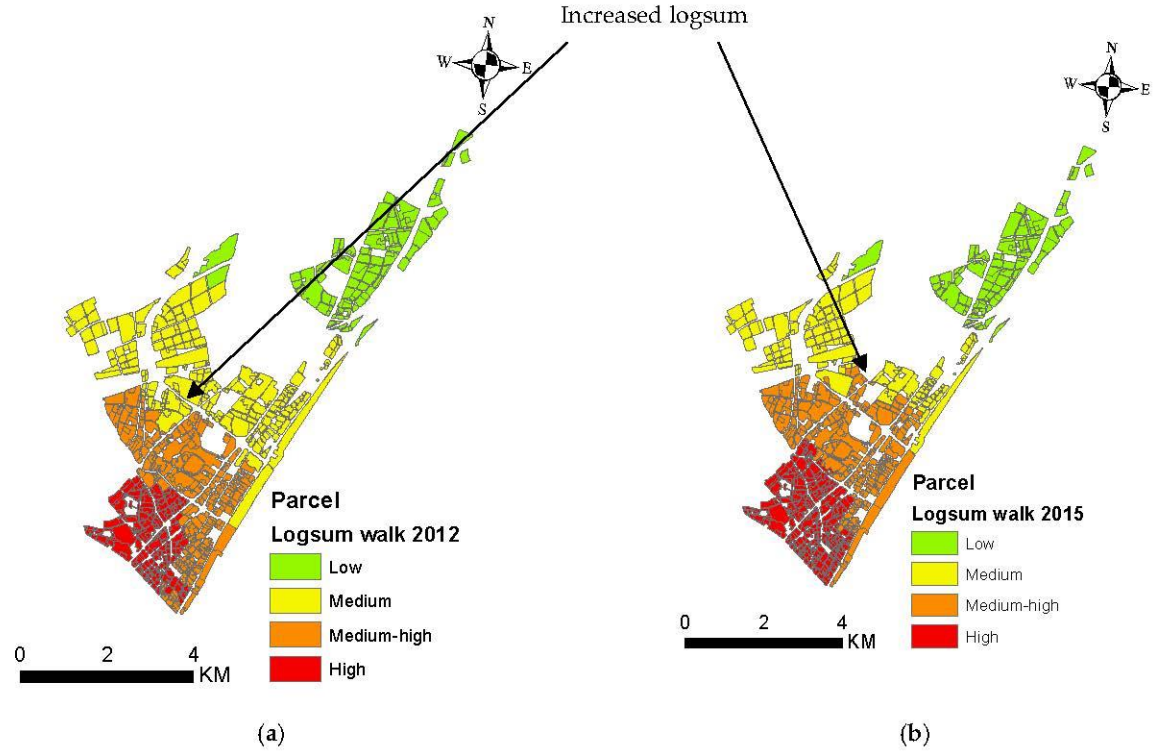


Figure 15. Logsum by walk at parcel level: (**a**) logsum by walk (2012); (**b**) logsum by walk (2015).

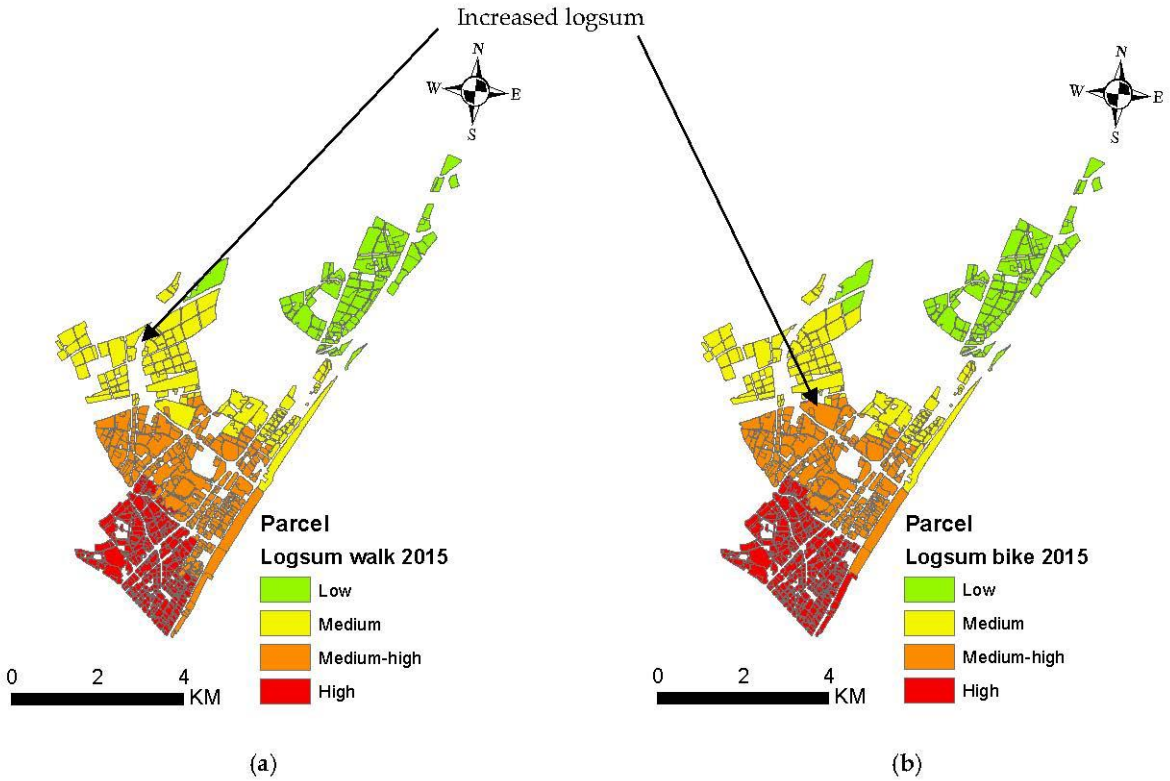


Figure 16. Logsum by bike at parcel level: (**a**) logsum by bike (2012); (**b**) logsum by bike (2015).

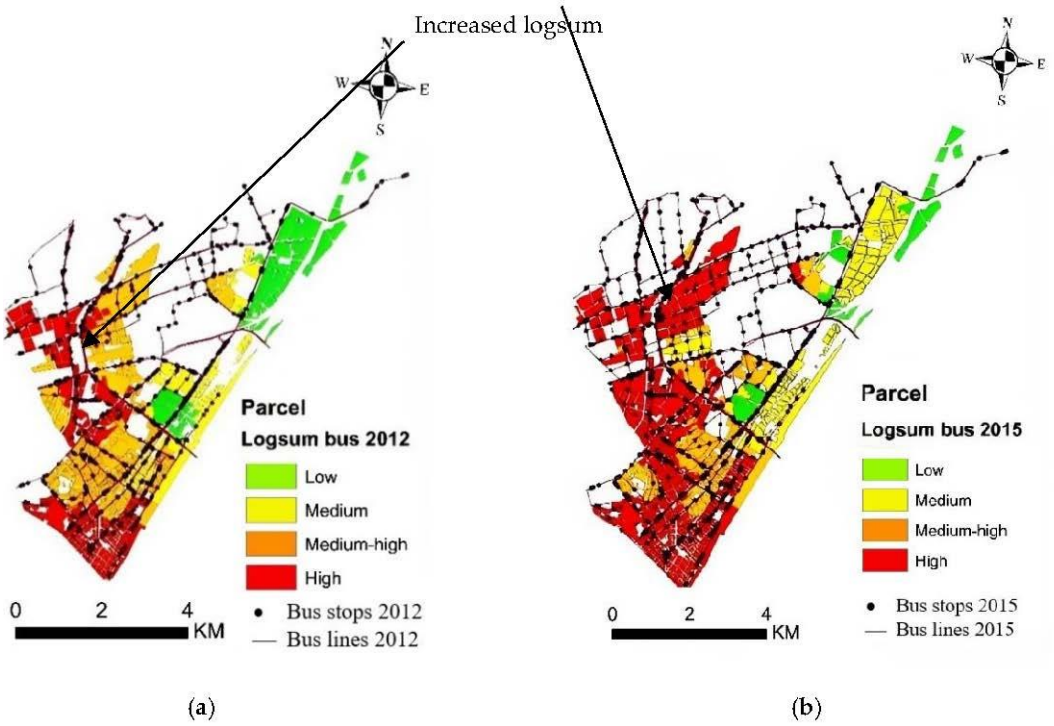


Figure 17. Logsum by bus at parcel level: (**a**) logsum by bus (2012); (**b**) logsum by bus (2015).

4.2.4. Logsum by Subway

Figure 18a,b depict the logsum by subway at the parcel level for the years 2012 and 2015. The results indicate that areas with high logsum values by subway correspond to a dense development of mixed (RC and CR) space quantities. In 2015, there was a notable increase in logsum values, particularly near subway line 1, leading to a significant rise in the mixed space quantity. These findings underscore a strong correlation between the logsum by subway and the mixed space quantity, attributed to the expansion of the subway infrastructure in Jiang'an District during the period from 2012 to 2015. In 2012, the District had only one subway line with 12 stations, but by 2015, the same line had expanded to 14 stations. Figure 18a,b show the index value range of the logsum by subway in 2012 and 2015: the lowest logsum (0.00~3.70) in the west of Jiang'an District, medium (3.71~4.21) in the center of Jiang'an District, medium-high (4.22~4.71) in the north of Jiang'an District, and the highest logsum (4.72~5.24) in the east and south of Jiang'an District, particularly close to subway line 1.

4.2.5. Logsum by Car

Figure 19a,b depict the logsum by car at the parcel level for the years 2012 and 2015. The results indicate that areas with a high logsum by car experience a dense development of residential spaces. Particularly in 2015, there was a significant increase in residential space development in parcels with high logsum values by car. These findings highlight a robust correlation between "the logsum by car" and developed spaces. Additionally, Figure 19a,b show the index value range of the logsum by car in 2012 and 2015: the lowest logsum (10.96~11.84), low-medium (11.85~13.54) in the north of Jiang'an District, medium (13.55~14.38) in the north and center of Jiang'an District, medium-high between (14.39~14.66) in the center of Jiang'an District, and the highest logsum (14.67~15.07) in the south of Jiang'an District.

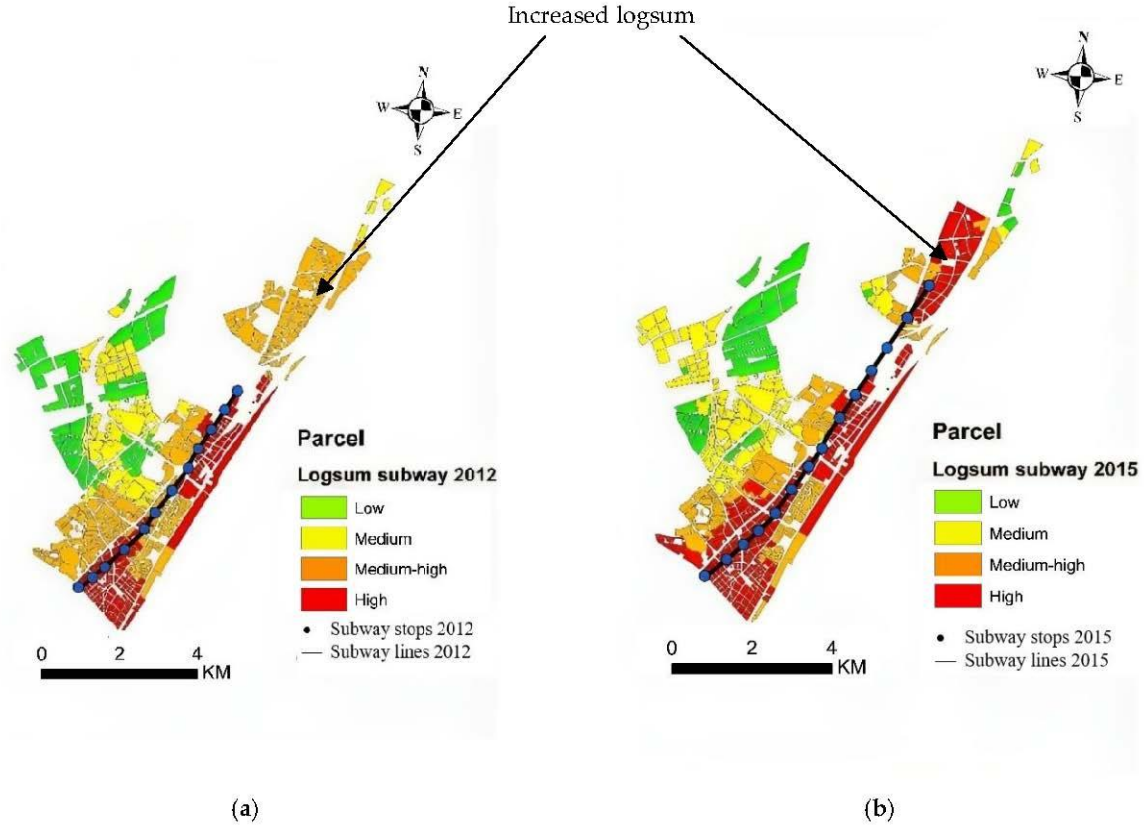


Figure 18. Logsum by subway at parcel level: (**a**) logsum by subway (2012); (**b**) logsum by subway (2015).

4.2.6. Logsum by Taxi

Figure 20a,b depict the logsum by taxi at the parcel level for the years 2012 and 2015. The results indicate that areas with high logsum values by taxi experience a dense development of commercial spaces. Particularly in 2015, there was a significant increase in commercial space development, especially along subway line 1 in the middle of Jiang'an District. These findings highlight a robust relationship between "the logsum by taxi" and the quantity of commercial space. Additionally, Figure 20a,b show the index value range of the logsum in 2012 and 2015: the lowest logsum (8.774~11.55) in the north of Jiang'an District, medium (11.56~12.97) in the center and north of Jiang'an District, medium-high (12.98~14.47) in the center of Jiang'an District, and the highest logsum by taxi (14.48~15.01) in the south of Jiang'an District.

Table 8 shows how the space quantities changed during the years 2012 to 2015,. For example, the total change in the commercial space quantity was 3,679,405 Sqr meters during the period from 2012 to 2015. Moreover, the total change in the mixed commercial–residential space quantity was recorded at 125,054 Sqr meters and the total change in te residential space quantity was 1,244,687 Sqr meters. Furthermore, the total change in the mixed residential–commercial space quantity was 451,688 Sqr meters. Figure 21a–d show the spatial density of the different space categories, revealing significant concentrations of developed residential, mixed (RC and CR), and commercial spaces. Particularly notable are the high-density areas located in the central and southern regions of Jiang'an District, near subway line 1 and the city center.

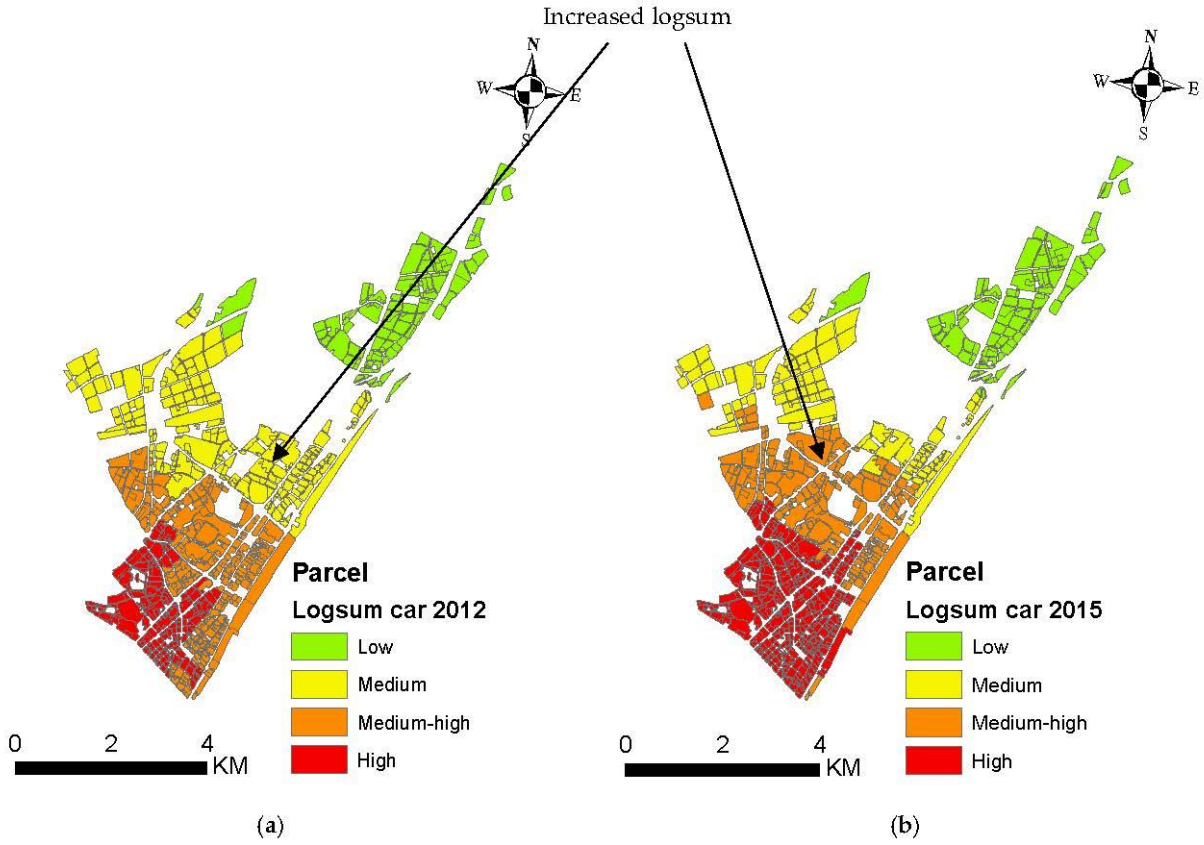


Figure 19. Logsum by car at parcel level: (**a**) logsum by car (2012); (**b**) logsum by car (2015).

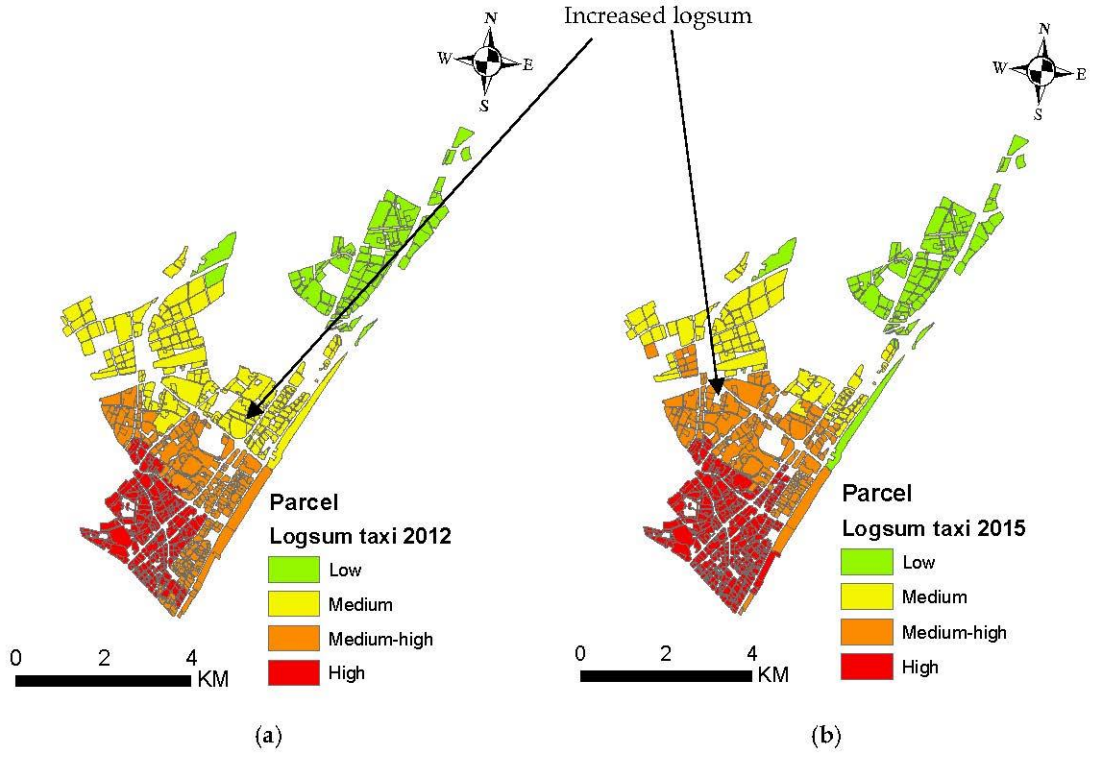


Figure 20. Logsum by taxi at parcel level: (**a**) logsum by taxi (2012); (**b**) logsum by taxi (2015).

Table 8. Total space quantity changes from 2012 to 2015 by parcel type.

Total of Space Quantity Change (m^2)					
Years/Type	**C**	**CR**	**R**	**RC**	**Total Space**
Total space quantity 2012	1,804,696	1,888,940	13,559,658	19,163,936	36,417,230
Total space quantity 2015	2,179,442	2,013,994	14,804,345	19,615,624	38,613,405
Total change	374,746	125,054	1,244,687	451,688	2,196,175

Note: R = residential, C = commercial, RC = mixed residential–commercial, CR = mixed commercial–residential, D = demolished, N = new development.

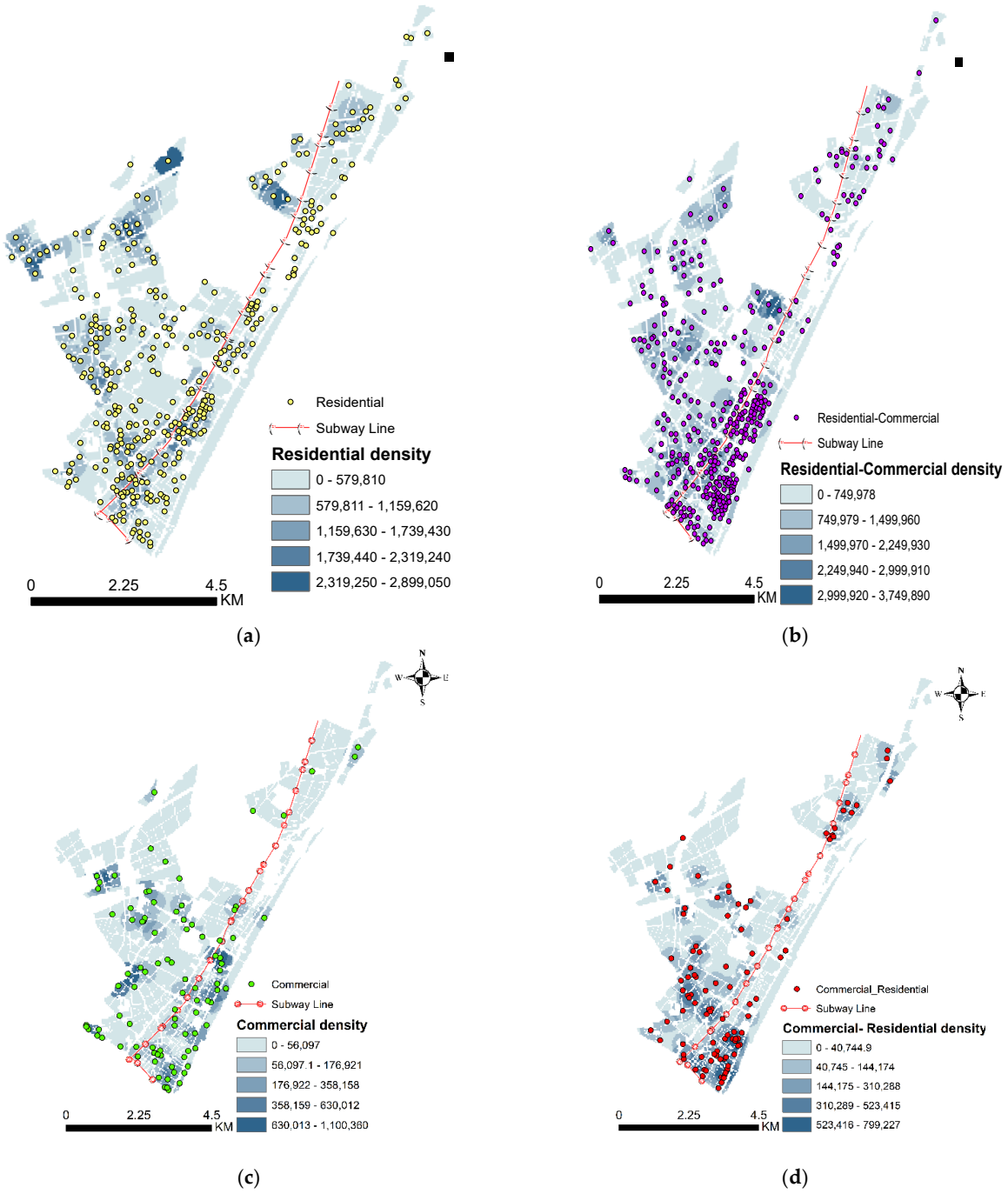


Figure 21. Density of space quantity by category: (**a**) residential density, (**b**) residential–commercial density, (**c**) commercial density, (**d**) commercial–residential density.

Figure 22 demonstrates a notable increase in the mixed commercial–residential and mixed residential–commercial spaces, with a rise of 451,688 and 125,054 square meters in 2012 and 2015, respectively. The areas along the subway line 1 had a high logsum in 2012 and 2015, particularly in the center of Jiang'an District. However, commercial and residential space has increased by 1,244,687 square meters and 374,746 square meters, respectively. Furthermore, the logsum from public transport (e.g., regular bus or subway) increased in 2015, indicating that the increased logsum from public transport encourages the development of mixed residential–commercial and residential spaces. However, it is found that it has little impact on the development of commercial and mixed commercial–residential spaces. A desirable commercial location should be close to main highways enabling the quicker movement of goods and services in order to meet customer demand.

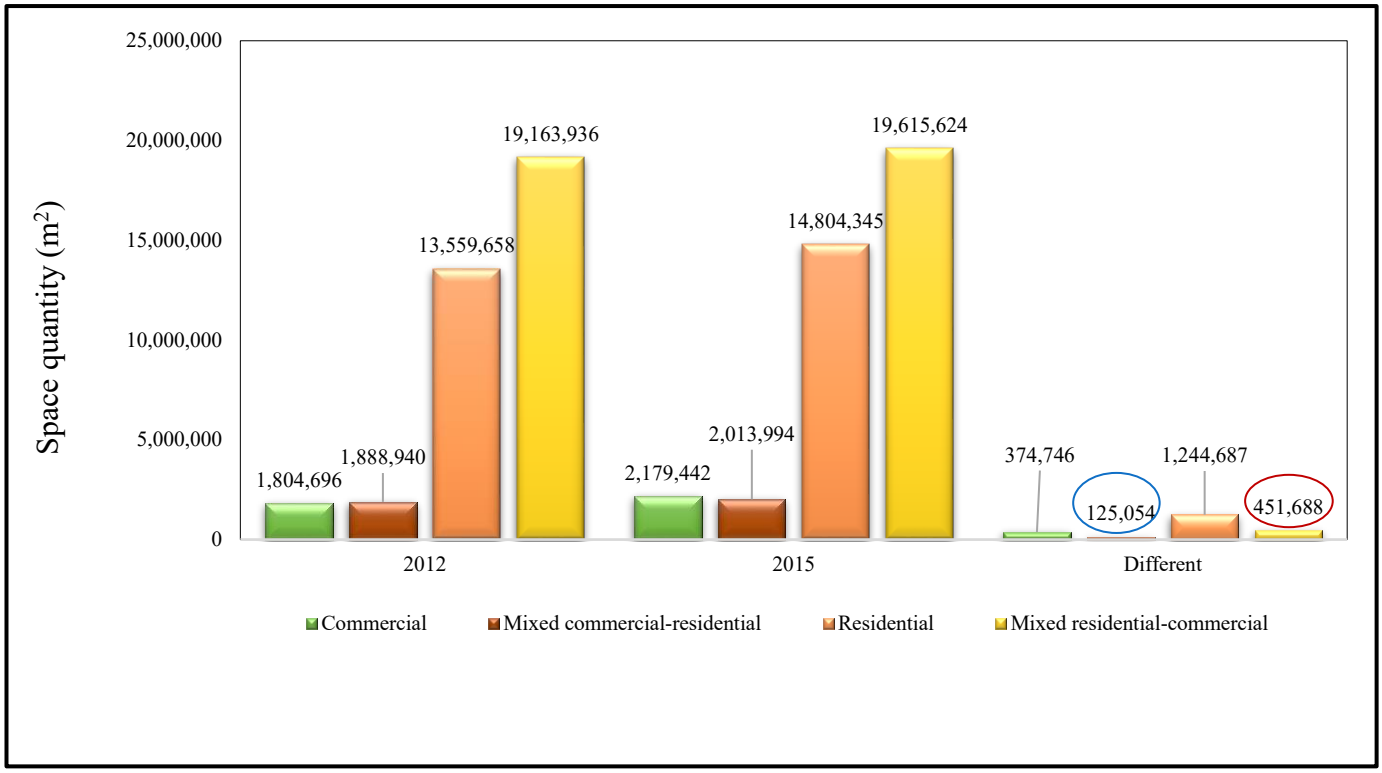


Figure 22. Total space quantity change comparison between 2012 and 2015.

The data was analyzed using two different MLU indexes: ENT and HH indexes, to measure the diversity and degree of land use. Figure 23a,b show the ENT index. The value range represents a high degree of MLU (0.057–0.69 and 0.58–0.69) a medium degree of MLU patterns (0.21–0.38 and 0.22–0.39), and a low degree of MLU patterns (0.010–0.20 and 0.010–0.21). The findings of the ENT index indicate that the majority of parcels have a high level of MLU density. Furthermore, Figure 23c,d show the HH index. The value range represents a high degree of MLU (50–57 and 50–58), a medium degree of MLU patterns (71–83), and a low degree of MLU patterns (84–99). Furthermore, a parcel with an ENT index of 0.0 and an HH index of 100 means a single type of land use. The HH index values in Figure 23c,d signifies that most parcels exhibit a high MLU level.

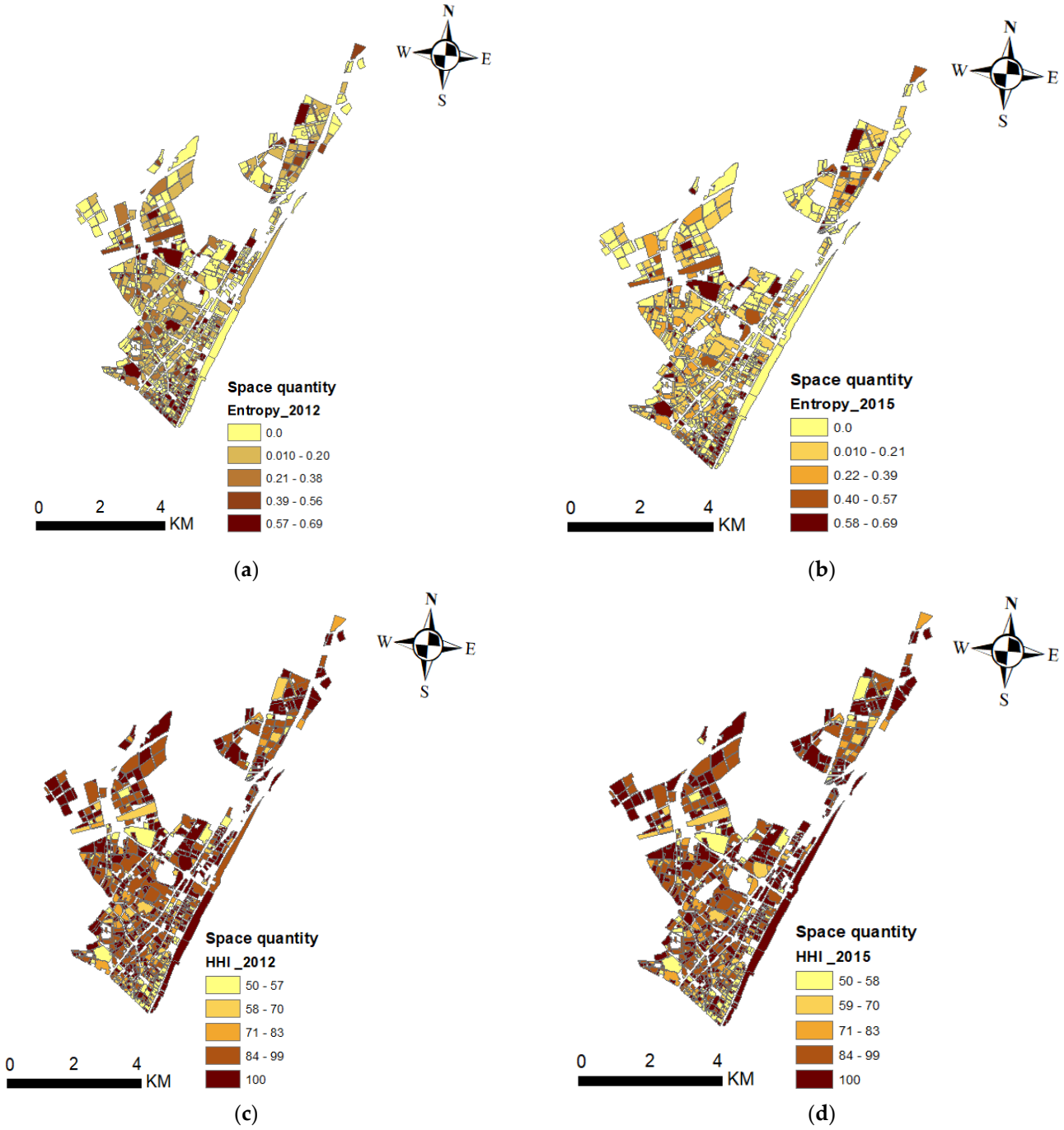


Figure 23. The entropy index and HH index for 2012 and 2015: (**a**) 2012 entropy index; (**b**) 2015 entropy index; (**c**) 2012 HH index; (**d**) 2015 HH index.

4.3. Parameter Settings and Model Training

As mentioned earlier in the second section—the Literature Review,—numerous factors, such as transport supply (represented by a logsum) and space prices, influence MLU density. The findings show that areas with a high-value logsum tend to have a high MLU density and vice versa [12,24,40]. Due to the nonlinear relationship among buildings, average space quantity, and logsum, this study, employs DNNs as the modeling tool, owing to their ability to effectively handle and analyze nonlinear data patterns [9]. In addition, the selected DNN (MLP, and LSTM) models, are designed to explore the relationship between the dependent variable, MLU pattern, and independent variables such as the logsum, maximum space development, and average floor space price. Python 3.12.0 software is utilized to develop

the network through Keras (Tensor Flow). The MLP and LSTM models are trained and tested using the input and output variables presented in Table 9.

Table 9. Input and output variables to the DNN models.

Input Variables for Training (70% of Data Samples)	Output Variables for Training (70% of Data Samples)	Input Variables for Testing (30% of Data Samples)	Output Variables for Testing (30% of Data Samples)
Average floor space price by types (2012, 2015) Maximum available space quantity Space quantity in 2012 Logsum by type (2012, 2015)	Space quantity in 2015, ENT index	Average floor space price by types (2012, 2015) Maximum available space quantity Space quantity in 2012 Logsum by type (2012, 2015)	Space quantity in 2015, ENT index

The MLP and LSTM models comprise ten layers. The first layer is the input layer which consists of 13 variables, including the logsum by mode for the years 2012 and 2015, space quantity in 2012, maximum available space quantity, and average floor space price for the years 2012 and 2015. The model also incorporates eight hidden layers to enhance the prediction accuracy while maintaining computational efficiency. The final output layer comprises two neurons, responsible for predicting the total quantity of MLU in a parcel and its ENT index. The ENT index represents the distribution of the different types of space quantities within a mixed development (e.g., 80% of residential and 20% of commercial).

The best parameter values are determined to be the following: batch size of 16 for training and 1026 for testing, learning rate of 0.001, 10,000 training epochs, and using stochastic gradient descent (SDG) optimization. The input layer consists of 13 variables, and the input layer neurons are set to 1000. The hidden layers range from 800 to 100 neurons, while the output layer ranges from 50 to 2 neurons. Additionally, missing data is carefully examined and outliers are thoroughly investigated and removed.

4.4. Results of Prediction Accuracy of the MLP and LSTM Models and Their Comparative Analysis

This study employs the MLP and LSTM to examine the influence of transportation infrastructure-based accessibility on the prevalence MLU patterns. In addition, the results of the MLP and LSTM models during the training and testing phases are utilized to evaluate the accuracy of each of them.

As mentioned in the above section, the Logsum is a measure, which is used to evaluate the level of supply of various transportation modes at a given location. This measure is, in turn, used to study its impact on the MLU patterns. Table 10 demonstrates the modes considered and their effect on MLU patterns under various scenarios. For instance, in the first scenario, the logsum of each of the solo mode (e.g., bike vs. car) is used to evaluate the effect of the supply of a specific mode on the MLU patterns. In the second scenario, the logsum based on all modes combined is used to evaluate the effect of transport supply from all available modes on the MLU patterns. In the third scenario, the logsum from the walk, bike, bus, and subway combined is used to evaluate the effect of their "combined" supply of public transit on the MLU patterns. In the fourth scenario, the logsum from the bus, subway, car, and taxi is used to evaluate the effect of the "combined" mobile transport supply on the MLU patterns. In the fifth scenario, only the nonmotorized (walk, bike) and auto (car, taxi) logsum is used to evaluate the effect of the supply of nonmotorized and auto transportation (car-dominant scenario) on the MLU patterns. In the sixth scenario, the logsum from the walk, bus, and car modes combined is used to evaluate their combined supply on the MLU patterns. Lastly, in the seventh scenario, the logsum from the bike, subway, and taxi combined is used to evaluate the "combined" supply of these modes on the MLU patterns.

Table 10. Analysis of the impact of different types of transport supply on MLU under different scenarios.

Mode /Scenario	Nonmotorized (Nmt)		Public Transit (Pt)		Auto	
Scenario 1 (All modes separated)	Walk	Bike	Bus	Subway	Car	Taxi
Scenario 2 (All modes together)	Walk	Bike	Bus	Subway	Car	Taxi
Scenario 3	Walk	Bike	Bus	Subway	---	---
Scenario 4	---	---	Bus	Subway	Car	Taxi
Scenario 5	Walk	Bike	---	---	Car	Taxi
Scenario 6	Walk	---	Bus	---	Car	---
Scenario 7	---	Bike	---	Subway	---	Taxi

Table 11 illustrates the supply of transport modes considered and their effect on the MLU patterns utilizing the MLP and LSTM models under various scenarios. In the training phase, the MLP mixed CR model results in a mean relative error (MRE) under the first scenario between 1.92 and 2.33, while under the scenarios 2, 3, 4, 5, 6, and 7, results in an MRE of 2.58, 3.70, 1.82, 1.42, 2.41, and 2.20, respectively. Based on the above results, the lowest MRE of the MLP mixed CR model is found to be 1.42 under scenario 5, which considers the "combined" transport supply of the following modes: walk, bike, car, and taxi mode. A lower MRE indicates a higher level of prediction accuracy. This finding shows that the MLP mixed CR model achieves its most accurate predictions under scenario 5, indicating that the combination of walk, bike, car, and taxi modes has a significant influence on mixed CR patterns. Additionally, this finding suggests that the model's predictions closely align with the actual observed values for mixed CR patterns in this scenario.

Table 11. Comparative analysis of the MLU predicting MRE of LSTM and MLP (training).

Models		MLP Training Errors (%)						LSTM Training Errors (%)					
Scenario\Land Type		Mixed CR MRE (%)			Mixed RC MRE (%)			Mixed CR MRE (%)			Mixed RC MRE(%)		
		C	R	CR	C	R	RC	C	R	CR	C	R	RC
Scenario 1	Walk	1.35	0.97	2.32	0.85	1.32	2.17	1.97	1.64	3.61	1.11	1.65	2.76
	Bike	1.36	0.97	2.33	0.84	1.31	2.15	1.99	1.66	3.65	1.12	1.66	2.78
	Bus	1.12	0.80	1.92	0.76	1.18	1.94	1.99	1.66	3.65	1.14	1.69	2.83
	Subway	1.34	0.96	2.30	0.74	1.15	1.89	1.78	1.48	3.26	1.10	1.64	2.74
	Car	1.35	0.97	2.32	0.83	1.30	2.13	2.07	1.72	3.79	1.12	1.67	2.79
	Taxi	1.36	0.97	2.33	0.84	1.31	2.15	2.02	1.68	3.70	1.13	1.68	2.81
Scenario 2		1.50	1.08	2.58	0.69	1.08	1.77	2.00	1.67	3.67	1.1	1.66	2.76
Scenario 3		2.16	1.54	3.70	0.67	1.05	1.72	1.98	1.65	3.63	1.12	1.66	2.78
Scenario 4		1.06	0.76	1.82	0.70	1.09	1.79	1.58	1.32	2.9	1.14	1.69	2.83
Scenario 5		0.83	0.59	1.42	1.08	1.69	2.77	2.12	1.76	3.88	1.11	1.64	2.75
Scenario 6		1.41	1.00	2.41	0.69	1.08	1.77	1.46	1.22	2.68	1.12	1.68	2.8
Scenario 7		1.28	0.92	2.20	0.71	1.12	1.83	2.04	1.70	3.74	1.09	1.62	2.71

Note: R = residential, C = commercial, RC = mixed residential–commercial, CR = mixed commercial–residential.

Moreover, in the training phase, the LSTM mixed CR model results in an MRE under the first scenario between 3.26 and 3.79, while the LSTM mixed CR model, under the scenarios 2, 3, 4, 5, 6, and 7, results in an MRE of 3.67, 3.63, 2.9, 3.88, 2.68, and 3.74, respectively. Based on the above results, the lowest MRE of the LSTM mixed CR model is found to be 2.68 under scenario 6, which considers the "combined" transport supply of the following modes: walk, bus, and car mode. The findings of the LSTM mixed CR model contradict to those of the MLP mixed CR model, as they demonstrate that the LSTM mixed CR model achieves the highest level of prediction accuracy under scenario 6, indicating

that the combination of walk, bus, and car modes has a significant influence on the mixed CR patterns.

Meanwhile, in the training phase, the MLP mixed RC models, under the first scenario, results in the MREs ranging between 1.89 and 2.17, whereas the MLP mixed RC model, under the scenarios 2, 3, 4, 5, 6, and 7, results in an MRE of 1.77, 1.72, 1.79, 2.77, 1.77, and 1.83, respectively. Based on the above results, the lowest MRE of the MLP mixed RC model is found to be 1.72 under scenario 3, which considers the effect of combined transport supply from the walk, bike, bus, and subway modes. This finding shows that the MLP mixed RC model achieves its most accurate predictions under scenario 3, indicating that the combination of walk, bike, bus, and subway modes has a significant influence on the mixed RC patterns.

On the other hand, in the training phase, the LSTM mixed RC models, under the first scenario, results in the MREs ranging between 2.74 and 2.83, whereas the LSTM mixed RC model, under the scenarios 2, 3, 4, 5, 6, and 7, results in an MRE of 2.76, 2.78, 2.83, 2.75, 2.8, and 2.71, respectively. Based on the above results, the lowest MRE of the LSTM mixed RC model is found to be 2.71 under scenario 7, which considers the effect of combined transport supply from the bike, subway, and taxi modes. The findings of the LSTM mixed RC model contradict those of the MLP mixed RC model, as they demonstrate that the LSTM mixed RC model achieves the highest level of prediction accuracy under scenario 7, indicating that the combination of bike, subway, and taxi modes has a significant influence on the mixed RC patterns.

The comparative findings of the LSTM and MLP in the testing phase are illustrated in Table 12. It also shows the modes considered and their effect on the MLU patterns utilizing the MLP and LSTM models for various scenarios. In the testing phase, the MLP mixed CR models results in an MRE under the first scenario between 8.53 and 9.42, whereas under scenarios 2, 3, 4, 5, 6, and 7, results in an MRE of 9.59, 14.08, 12.61, 10.21, 7.78, and 7.30, respectively. Based on the above results, the lowest MRE of the MLP mixed CR model is found to be 7.30 under scenario 7, which considers the "combined" transport supply of the following modes: bike, subway, and taxi mode. A lower MRE signifies a higher level of prediction accuracy. This finding shows that the MLP mixed CR model achieves its most accurate predictions under scenario 7, indicating that the combination of bike, subway, and taxi modes has a significant influence on mixed CR patterns.

Table 12. Comparative analysis of the MLU predicting errors (testing).

Models		**MLP Testing Errors (%)**						**LSTM Testing Errors (%)**					
MRE		**Mixed CR MRE (%)**			**Mixed RC MRE (%)**			**Mixed CR MRE (%)**			**Mixed RC MRE (%)**		
Scenario\Land Type		**C**	**R**	**CR**	**C**	**R**	**RC**	**C**	**R**	**CR**	**C**	**R**	**RC**
Scenario 1	Walk	5.61	3.50	9.11	3.57	2.61	6.18	4.43	3.09	7.52	1.7	2.30	4
	Bike	5.57	3.48	9.05	3.43	2.50	5.93	4.34	3.03	7.37	1.80	2.30	4.10
	Bus	5.25	3.28	8.53	3.52	2.57	6.09	5.58	3.89	9.47	1.72	2.20	3.92
	Subway	5.80	3.62	9.42	3.55	2.59	6.14	5.58	3.89	9.47	1.81	2.31	4.12
	Car	5.54	3.46	9.00	3.51	2.56	6.07	4.49	3.14	7.63	1.85	2.36	4.21
	Taxi	5.51	3.44	8.95	3.48	2.54	6.02	4.39	3.07	7.46	1.85	2.37	4.22
Scenario 2		5.90	3.69	9.59	2.78	2.03	4.81	4.76	3.32	8.08	1.93	2.47	4.40
Scenario 3		8.67	5.41	14.08	2.72	1.98	4.70	5.54	3.87	9.41	1.94	2.48	4.42
Scenario 4		7.76	4.85	12.61	2.74	2.00	4.74	5.10	3.56	8.66	2.00	2.55	4.55
Scenario 5		6.29	3.92	10.21	3.16	2.31	5.47	6.11	4.27	10.38	1.92	2.45	4.37
Scenario 6		4.79	2.99	7.78	2.87	2.09	4.96	4.59	3.20	7.79	1.64	2.10	3.74
Scenario 7		4.49	2.81	7.30	3.02	2.20	5.22	4.19	2.92	7.11	2.01	2.57	4.58

On the other hand, in the testing phase, the LSTM mixed CR models result in an MRE under the first scenario between 7.37 and 9.47, whereas the LSTM mixed CR models under scenarios 2, 3, 4, 5, 6, and 7, results in an MRE of 8.08, 9.41, 8.66, 10.38, 7.79, and 7.11,

respectively. Based on the above results, the lowest MRE of the LSTM mixed CR model is found to be 7.11 under scenario 7, which considers the "combined" transport supply of the following modes: bike, subway, and taxi mode. Similar to the MLP model, the LSTM model also shows the same results for the mixed CR model, indicating that it achieves its most accurate predictions under scenario 7. This suggests that the combination of bike, subway, and taxi modes has a significant influence on mixed CR patterns. Meanwhile, in the testing phase of the MLP mixed RC models, under the first scenario, results in the MREs ranging between 5.93 and 6.18, whereas the MLP mixed RC model, under the scenarios 2, 3, 4, 5, 6, and 7, results in MRE of 4.81,4.70, 4.74, 5.47, 4.96, and 5.22, respectively. Based on the above results, the lowest MRE of the MLP mixed RC model is found to be 4.70 under scenario 3, which considers the effect of combined transport supply from the walk, bike, bus, and subway modes. This finding shows that the MLP mixed RC model achieves its most accurate predictions under scenario 3, indicating that the combination of walk, bike, bus, and subway modes has a significant influence on the mixed RC patterns.

Meanwhile, in the testing phase of the LSTM mixed RC models, under the first scenario, results in MREs ranging between 3.92 and 4.22, whereas the LSTM mixed RC model, under the scenarios 2, 3, 4, 5, 6, and 7, results in an MRE of 4.4, 4.42, 4.55, 4.37, 3.74, and 4.58, respectively. Based on the above results, the lowest MRE of the LSTM mixed RC model is found to be 3.74 under scenario 6, which considers the effect of combined transport supply from the walk, bus, and car modes. The findings of the LSTM mixed RC model contradict those of the MLP mixed RC model. The LSTM mixed RC model demonstrates the highest level of prediction accuracy under scenario 6, indicating that the combination of walk, bus, and car modes has a significant influence on the mixed RC patterns.

4.5. Discussion

The primary objective of this research is to analyze the influence of transportation infrastructure-based accessibility on the prevalence of MLU patterns. The study focuses on Jiang'an District, Wuhan, China, examining data from the years 2012 and 2015 to illustrate this process. The proposed model used DNN approaches such as MLP and LSTM. This study uses several MLU types (such as mixed residential–commercial and mixed commercial–residential), the logsum by different modes under several different scenarios (walk, bike, bus, subway, car, and taxi), and the average floor space prices (such as commercial and residential).

The study results show that the majority of parcels with residential and mixed residential–commercial land use patterns changed considerably by 451,688 Sqr meters and 1,244,687 Sqr meters, respectively, for the years 2012 and 2015, in areas that had a high logsum under scenario 3 (walk, bike, bus, subway) and scenario 6 (walk, bus, car) with the MRE of the MLP and LSTM (4.7% and 3.74%), respectively, in the area close to the city center, as well as in the center and south of Jiang'an District. However, the amount of mixed commercial–residential and commercial area has increased primarily in the areas around the subway line 1 by 125,054 Sqr meters and 374,746 Sqr meters with a high logsum under scenario 7 (bike, subway, taxi), with an MRE of 7.3% for the MLP and 7.11% for the LSTM. This means that the increased logsum under scenario 3 (walk, biking, bus, subway) encourages mixed residential–commercial and residential space development. Moreover, the rise in the logsum values under scenario 7 (bike, subway, taxi) promotes the development of mixed commercial–residential and commercial spaces. Both the MLP and LSTM models highlight a significant correlation between public transport supply and MLU development. In addition, the findings from the CLD show that there is a causal relationship between transportation supply, MLU, population, employment, and housing price. Furthermore, an increase in the access to retail and other services, in the city center, is likely to lead to a rise in floor space prices. Additionally, rising floor space prices may result in an increase in MLU developments.

Based on the study results, it is evident that parcels with high logsum values often correspond to high MLU patterns, whereas those with low logsum values tend to be

associated with lower MLU patterns. The findings of the MLP and LSTM models indicate an MRE of 4.7–14.08% and 3.74–10.38%, respectively. The findings of previous studies are shown in Table 13, which also used the machine learning approaches, i.e., the decision tree model, to examine the influence of accessibility on MLU. For instance, a study conducted by Jayasinghe et al. [12] illustrates that areas with high accessibility exhibit a dense MLU pattern, while low-accessibility areas show a sparse MLU pattern, which is consistent with our study findings. On the other hand, the decision tree model results showed an MRE of 20%, which is six times higher than that of our MLP model and twice as high as our LSTM model. Furthermore, Wu et al. [11] introduced a multi-label convolutional neural network (ML-CNN-CA) model employing a multi-label learning strategy to simulate the changes in MLU. Their results showed that the proportion of MLU cells in total land use areas increased from 2009 (16.03%) to 2013 (16.87%), and reached 17% in 2020. Considering the growing trend observed in most MLU cells, it is anticipated that the dynamic of MLU will continue to increase in subsequent years. Consequently, the ML-CNN-CA model proves to be an efficient method for simulating changes in the MLU pattern and their model's yield MRE of 9–11%. Likewise, Yang et al. [8] employed the MGWR and ENT index to analyze the spatial distribution and aggregation characteristics of the MLU. It was determined in the city of Beijing that the MLU level is higher in the city center, where accessibility is higher, and lower in the city's suburbs, where the accessibility is lower. Their models result in an MRE of 17.33%. Moreover, He et al. [56] use a two-branch CNN for combining features (CF-CNN) that consists of a simplified residual network (SRes-Net) and a modified visual geometry group network (PVGG-Net) to extract information from remote sensing imagery data and Tencent user density for human activity-related information extraction to estimate the proportion of MLU in the city of Guangzhou. Their findings revealed that residential and commercial zones are concentrated in the study area's center, while industrial zones and green space are located near the edges of the suburbs. Mixed land use can reduce the community distance and increase neighborhood vibrancy. Their models yield an MRE of 6% (CF-CNN), 8.3% (SRes-Net), and 10% (PVGG-Net). The outcomes of those studies showed that accessibility and MLU has a strong correlation and co-existence relationship. These results also show that the models developed in this study are better for forecasting the MLU patterns, in terms of their forecasting accuracy.

Table 13. Comparison of the forecasting error between previous studies and the current study.

Authors	Objectives	Methodology	City/ Country	MRE
Jayasinghe et al. [12]	Analyze the relationship between accessibility, MLU, and densities	Decision tree	Srilanka	20%
Yang et al. [8]	Explore the impact of accessibility and MLU on housing price	MGWR	Beijing, China	17.33%
Wu et al. [11]	A study on cellular automata with machine learning to simulate MLU changes	(ML-CNN-CA)	Huizhou, China	9–11%
He et al. [56]	Estimate the percentage of MLU changes using DNN (CNN)	(CF-CNN), (SRes-Net), (PVGG-Net)	Guangzhou, China	6%, 8.3%, and 10%
The proposed model of the current study	Evaluate the effect of transport supply on MLU at the parcel level	MLP and LSTM	Wuhan, China	4.7–14.08% and 3.74–10.38%

5. Conclusions and Recommendations

This study adopted state-of-the-art DNN techniques, such as MLP and LSTM models to investigate the impact of transportation infrastructure-based accessibility on the prevalence of MLU patterns at the parcel level. The study focuses on the Jiang'an District in Wuhan, China, as a case study, and utilized data for the years 2012 and 2015. The data used in this study includes several types of logsum, MLU patterns at the parcel level, and floor space prices by space type, for the years 2012 and 2015. The ENT and HH indexes are utilized to measure the degree of MLU at each parcel. Based on the study results of this paper, the following conclusions can be drawn:

According to the results of this study, parcels with a high logsum by the walking mode, such as those under the scenario 1 (4.17~4.32), have a high level of MLU patterns.

- The study findings indicate significant changes in land use patterns, particularly in residential and mixed residential–commercial parcels, between 2012 and 2015. These changes were most pronounced in areas characterized by high logsum values under scenarios 3 (walk, bike, bus, subway) and 6 (walk, bus, car) in the central and southern regions of Jiang'an District. However, the amount of commercial and mixed commercial–residential area has increased primarily in the areas around the subway line 1 with a high logsum under scenario 7 (bike, subway, taxi). This implies that the increased logsum due to the supply of public transit under scenario 3 (walk, bike, bus, subway) and scenario 6 (walk, bus, car) encourages residential and mixed residential–commercial land development. Also, the increased logsum under scenario 7 (bike, subway, taxi) encourages commercial and mixed commercial–residential land development. The results from this study reinforced the conclusions from the previous studies that there is a strong relationship between transport supply and MLU.
- The ENT and HH indexes, which are used to represent the level of MLU, show that the spatial distribution of a high and medium MLU density are increasingly found in downtown areas and around subway line 1, while areas farther away from the city center have a low MLU density for the years 2012 and 2015, suggesting that policies should be devised to enhance transport supply (represented by the logsum in the model) to encourage a high MLU density.
- The MLP and LSTM model's results indicated an MRE of 4.7–14.08%, and 3.74–10.38%, respectively. These findings indicate that the LSTM model outperforms the MLP model for all types of MLU.
- This study employed a parcel-level disaggregated land use data to explore the relationship between transport supply and MLU patterns. This approach offers a nuanced understanding of land use dynamics, providing a more precise depiction of land development. Such detailed analysis significantly enhances the utility of the study's findings in policy analysis. Using parcel-level data could help the government, stakeholders, and regional planning agencies in distributing measured demand across parcels in a manner reflective of differences in land use and intensity. With demand assigned to individual parcels, it is possible to determine the effects of a fluctuating transport supply on MLU. In fact, the method can be used to assess both new development plans and the existing urban fabric.
- This paper employs real-world data and considers the case of a developing country to evaluate the relationship between transport supply and MLU. This will provide some guidelines and directions for the development of MLU and smart city in developing countries.
- To promote and regulate MLU in urban zones, planners can develop a set of regulations regarding required transport supply measures. In addition, the technique can be applied to efficiently develop planning and land use regulations.
- Examining the relationship between accessibility and MLU in urban settings empowers urban and transport planners to shape spatial conditions, fostering urban diversity, thereby contributing to desired sustainability. This approach not only guides the

evolution of the city but also offers a framework for overseeing existing areas where MLU density requires management.

- The study reveals that the density of MLU is intricately linked to the accessibility of subways and the city center. Consequently, effective planning and zoning regulations are essential to facilitate natural urban development instead of artificially dictating its form. Decision-makers can leverage these study findings to strategically intervene and realize the envisioned urban structure.
- The study's insights can be applied to model MLU based on specific accessibility scenarios. Moreover, it directly informs interventions in transport and town planning, aiding in understanding how changes in accessibility impact MLU. In essence, the study concludes that this serves as a valuable tool for decision-makers in town planning, land use planning, and transport planning, all aimed at achieving the overarching sustainability of future cities.
- This study used advanced DNN techniques to predicts the impact of transportation-accessibility on MLU patterns at the parcel level. These insights empower long-term town planning through optimized urban predictions, informed accessibility planning, tailored policy formulation, and scenario modeling. By understanding the intricate relationship between accessibility and MLU density, decision-makers can guide sustainable urban growth, ensuring cities evolve harmoniously and inclusively.

The proposed models from this study are only tested based on the data from a district in the city of Wuhan, China, which may or may not be applicable to other contexts. Therefore, planning agencies in other contexts are encouraged to test the methods provided within this study in their real-world land use modeling/planning process. Furthermore, the absence of MLU data spanning multiple years hampers the ability to conduct a comprehensive analysis comparing land use changes with variations in transport supply over an extended period. To conduct a thorough study, additional data is essential. This includes comprehensive information to construct a versatile model for mixed-space patterns, as well as examining the impact of the density, floor space price, and logsum on MLU patterns. The forthcoming study should also incorporate social aspects such as the safety and security of the region, urban space quality, livability, air quality conditions, and regulations/policies in the context of MLU. In developing nations, acquiring up-to-date parcel data and yearly building data presents a formidable challenge. Additionally, transport planning and household surveys in developing nations are typically conducted every 8 to 10 years due to the substantial investment and resources required. As the temporal continuum unfolds, the progressive evolution of information technology has endowed us with innovative avenues for the acquisition of pivotal data and the deployment of state-of-the-art tools. Our future research intends to tackle the mentioned shortcomings as soon as the requisite and up-to-date data becomes accessible.

Author Contributions: Conceptualization, Y.A., M.Z., M.S. and A.R.; Methodology, Y.A., M.Z., M.S., A.R., A.D. and M.A.A.A.-q.; Software, Y.A., M.S., A.R., A.D. and M.A.A.A.-q.; Validation, Y.A., M.Z., M.S. and A.R.; Formal analysis, M.Z. and M.S.; Investigation, M.Z.; Resources, M.Z.; Data curation, Y.A. and M.Z.; Writing—original draft, Y.A., M.Z., M.S. and A.R.; Writing—review & editing, M.Z. and M.S.; Visualization, M.S.; Supervision, M.Z.; Project administration, M.Z.; Funding acquisition, M.Z. All authors have read and agreed to the published version of the manuscript.

Funding: This research was funded by the National Natural Science Foundation of China: (Grant no. 52172309).

Institutional Review Board Statement: Not applicable.

Informed Consent Statement: Not applicable.

Data Availability Statement: The corresponding author can provide the data upon reasonable request.

Conflicts of Interest: The authors declare no conflict of interest.

References

1. Safdar, M.; Jamal, A.; Al-Ahmadi, H.M.; Rahman, M.T.; Almoshaogeh, M. Analysis of the Influential Factors towards Adoption of Car-Sharing: A Case Study of a Megacity in a Developing Country. *Sustainability* **2022**, *14*, 2778. [CrossRef]
2. Nabil, N.A.; Abd Eldayem, G.E. Influence of mixed land-use on realizing the social capital. *HBRC J.* **2015**, *11*, 285–298. [CrossRef]
3. Knorre, A.; MacDonald, J. Shootings and land use. *J. Crim. Justice* **2023**, *86*, 102068. [CrossRef]
4. Burton, E. Measuring Urban Compactness in UK Towns and Cities. *Environ. Plan. B Plan. Des.* **2002**, *29*, 219–250. [CrossRef]
5. Association, A.P. *Policy Guide on Smart Growth*; The Association: Chicago, IL, USA, 2002.
6. Sultana, S.; Powell, W.; Grant, J. Planning the Good Community: New Urbanism in Theory and Practice (review). *Southeast. Geogr.* **2009**, *49*, 308–312. [CrossRef]
7. Shi, B.; Yang, J. Scale, distribution, and pattern of mixed land use in central districts: A case study of Nanjing, China. *Habitat Int.* **2015**, *46*, 166–177. [CrossRef]
8. Yang, H.; Fu, M.; Wang, L.; Tang, F. Mixed Land Use Evaluation and Its Impact on Housing Prices in Beijing Based on Multi-Source Big Data. *Land* **2021**, *10*, 1103. [CrossRef]
9. Choi, D.; Kang, M.; Yoon, J. Utility of mixed-use development by reducing aggregated travel time for multiple non-work activities: A case of Seoul, Korea. *Cities* **2021**, *109*, 103007. [CrossRef]
10. Liang, X.; Guan, Q.F.; Clarke, K.C.; Chen, G.Z.; Guo, S.; Yao, Y. Mixed-cell cellular automata: A new approach for simulating the spatio-temporal dynamics of mixed land use structures. *Landsc. Urban Plan.* **2021**, *205*, 103960. [CrossRef]
11. Wu, X.; Liu, X.; Zhang, D.; Zhang, J.; He, J.; Xu, X. Simulating mixed land-use change under multi-label concept by integrating a convolutional neural network and cellular automata: A case study of Huizhou, China. *GIScience Remote Sens.* **2022**, *59*, 609–632. [CrossRef]
12. Jayasinghe, A.; Madusanka, N.B.S.; Abenayake, C.; Mahanama, P.K.S. A Modeling Framework: To Analyze the Relationship between Accessibility, Land Use and Densities in Urban Areas. *Sustainability* **2021**, *13*, 467. [CrossRef]
13. Peng, Y.; Yamaguchi, H.; Funabora, Y.; Doki, S. Modeling Fabric-Type Actuator Using Point Clouds by Deep Learning. *IEEE Access* **2022**, *10*, 94363–94375. [CrossRef]
14. Peng, Y.; Li, D.; Yang, X.; Ma, Z.; Mao, Z. A Review on Electrohydrodynamic (EHD) Pump. *Micromachines* **2023**, *14*, 321. [CrossRef] [PubMed]
15. Wu, C.; Pei, Y.; Gao, J. Model for Estimation Urban Transportation Supply-Demand Ratio. *Math. Probl. Eng.* **2015**, *2015*, 502739. [CrossRef]
16. Cao, R. Multi-Source Data Fusion for Land Use Classification Using Deep Learning. Ph.D. Thesis, University of Nottingham, Nottingham, UK, 2021. Available online: http://eprints.nottingham.ac.uk/63100/ (accessed on 5 October 2023).
17. Kudas, D.; Wnęk, A.; Tátošová, L. Land Use Mix in Functional Urban Areas of Selected Central European Countries from 2006 to 2012. *Int. J. Environ. Res. Public Health* **2022**, *19*, 15233. [CrossRef] [PubMed]
18. Ren, F.; Zhang, J.; Yang, X. Study on the Effect of Job Accessibility and Residential Location on Housing Occupancy Rate: A Case Study of Xiamen, China. *Land* **2023**, *12*, 912. [CrossRef]
19. Li, J.; Huang, H. Effects of transit-oriented development (TOD) on housing prices: A case study in Wuhan, China. *Res. Transp. Econ.* **2020**, *80*, 100813. [CrossRef]
20. Seong, E.Y.; Lee, N.H.; Choi, C.G. Relationship between Land Use Mix and Walking Choice in High-Density Cities: A Review of Walking in Seoul, South Korea. *Sustainability* **2021**, *13*, 810. [CrossRef]
21. Kim, D.; Jin, J. The Effect of Land Use on Housing Price and Rent: Empirical Evidence of Job Accessibility and Mixed Land Use. *Sustainability* **2019**, *11*, 938. [CrossRef]
22. Bhattacharjee, S.; Goetz, A.R. The rail transit system and land use change in the Denver metro region. *J. Transp. Geogr.* **2016**, *54*, 440–450. [CrossRef]
23. Van Nes, A.; Berghauser Pont, M.; Mashhoodi, B. Combination of Space syntax with spacematrix and the mixed use index: The Rotterdam South test case. In Proceedings of the 8th International Space Syntax Symposium, Santiago de Chile, Chile, 3–6 January 2012; Available online: http://resolver.tudelft.nl/uuid:d865e5b6-519e-4959-8c3d-800054d1b351 (accessed on 20 October 2023).
24. Koster, H.R.A.; Rouwendal, J. The Impact of Mixed Land Use on Residential Property Values*. *J. Reg. Sci.* **2012**, *52*, 733–761. [CrossRef]
25. Maithani, S. A neural network based urban growth model of an Indian city. *J. Indian Soc. Remote Sens.* **2009**, *37*, 363–376. [CrossRef]
26. Bivina, G.R.; Gupta, A.; Parida, M. Influence of microscale environmental factors on perceived walk accessibility to metro stations. *Transp. Res. Part D Transp. Environ.* **2019**, *67*, 142–155. [CrossRef]
27. Munshi, T. Accessibility, Infrastructure Provision and Residential Land Value: Modelling the Relation Using Geographic Weighted Regression in the City of Rajkot, India. *Sustainability* **2020**, *12*, 8615. [CrossRef]
28. Peng, Z.-R.; Zhao, L.-Y.; Yang, F. *Development of a Prototype Land Use Model for Statewide Transportation Planning Activities*; University of Florida: Gainesville, FL, USA, 2011. Available online: https://rosap.ntl.bts.gov/view/dot/23704 (accessed on 4 October 2023).
29. Raman, R.; Roy, U.K. Taxonomy of urban mixed land use planning. *Land Use Policy* **2019**, *88*, 104102. [CrossRef]
30. Almansoub, Y.; Zhong, M.; Raza, A.; Safdar, M.; Dahou, A.; Al-qaness, M.A.A. Exploring the Effects of Transportation Supply on Mixed Land-Use at the Parcel Level. *Land* **2022**, *11*, 797. [CrossRef]
31. Raza, A.; Safdar, M.; Zhong, M.; Hunt, J.D. Analyzing Spatial Location Preference of Urban Activities with Mode-Dependent Accessibility Using Integrated Land Use–Transport Models. *Land* **2022**, *11*, 1139.

32. Aygoren, S. Ins and Outs of Mixed-Use. *Real Estate Forum* **2004**, *59*, 66–71. Available online: https://www.cnu.org/sites/default/files/mixed_use_final_report_1-14-13_0.pdf (accessed on 3 October 2023).
33. Hoppenbrouwer, E.; Louw, E. Mixed-use development: Theory and practice in Amsterdam's Eastern Docklands. *Eur. Plan. Stud.* **2005**, *13*, 967–983. [CrossRef]
34. Thwaites, K.; Porta, S.; Romice, O.; Greaves, M. *Urban Sustainability through Environmental Design*; Routledge: Abingdon, VA, USA, 2007; p. 166. Available online: https://www.planninginsights.co.in/data/ebook/1625738019.pdf (accessed on 20 October 2023).
35. Maerten, A.-S.; Soydaner, D. From paintbrush to pixel: A review of deep neural networks in AI-generated art. *arXiv* **2023**, arXiv:2302.10913. [CrossRef]
36. Rodriguez-Conde, I.; Campos, C.; Fdez-Riverola, F. Horizontally Distributed Inference of Deep Neural Networks for AI-Enabled IoT. *Sensors* **2023**, *23*, 1911. [CrossRef] [PubMed]
37. Lopez-Ballester, J.; Felici-Castell, S.; Segura Garcia, J.; Cobos, M. AI-IoT Platform for Blind Estimation of Room Acoustic Parameters Based on Deep Neural Networks. *IEEE Internet Things J.* **2022**, *10*, 855–866. [CrossRef]
38. Omrani, H.; Tayyebi, A.; Pijanowski, B. Integrating the multi-label land-use concept and cellular automata with the artificial neural network-based Land Transformation Model: An integrated ML-CA-LTM modeling framework. *GIScience Remote Sens.* **2017**, *54*, 283–304. [CrossRef]
39. Zhao, Y.; Lin, Q.W.; Ke, S.G.; Yu, Y.H. Impact of land use on bicycle usage: A big data-based spatial approach to inform transport planning. *J. Transp. Land Use* **2020**, *13*, 299–316. [CrossRef]
40. Qin, Z.J.; Yu, Y.; Liu, D.F. The Effect of HOPSCA on Residential Property Values: Exploratory Findings from Wuhan, China. *Sustainability* **2019**, *11*, 471. [CrossRef]
41. Kaeoruean, K.; Phithakkitnukoon, S.; Demissie, M.G.; Kattan, L.; Ratti, C. Analysis of demand–supply gaps in public transit systems based on census and GTFS data: A case study of Calgary, Canada. *Public Transp.* **2020**, *12*, 483–516. [CrossRef]
42. Rad, T.G.; Alimohammadi, A. Modeling relationships between the network distance and travel time dynamics for assessing equity of accessibility to urban parks. *Geo-Spat. Inf. Sci.* **2021**, *24*, 509–526. [CrossRef]
43. Sungwon, L.; Bumsoo, L. Comparing the impacts of local land use and urban spatial structure on household VMT and GHG emissions. *J. Transp. Geogr.* **2020**, *84*, 102694. [CrossRef]
44. Jiao, J.C.; Rollo, J.; Fu, B.B. The Hidden Characteristics of Land-Use Mix Indices: An Overview and Validity Analysis Based on the Land Use in Melbourne, Australia. *Sustainability* **2021**, *13*, 1898. [CrossRef]
45. Hu, W.; Dong, J.; Hwang, B.-g.; Ren, R.; Chen, Y.; Chen, Z. Using system dynamics to analyze the development of urban freight transportation system based on rail transit: A case study of Beijing. *Sustain. Cities Soc.* **2020**, *53*, 101923. [CrossRef]
46. Fontoura, W.B.; Chaves, G.d.L.D.; Ribeiro, G.M. The Brazilian urban mobility policy: The impact in São Paulo transport system using system dynamics. *Transp. Policy* **2019**, *73*, 51–61. [CrossRef]
47. Song, Y.; Merlin, L.; Rodriguez, D. Comparing measures of urban land use mix. *Comput. Environ. Urban Syst.* **2013**, *42*, 1–13. [CrossRef]
48. Frank, L.D.; Schmid, T.L.; Sallis, J.F.; Chapman, J.; Saelens, B.E. Linking objectively measured physical activity with objectively measured urban form—Findings from SMARTRAQ. *Am. J. Prev. Med.* **2005**, *28*, 117–125. [CrossRef]
49. Ienco, D.; Gaetano, R.; Dupaquier, C.; Maurel, P. Land Cover Classification via Multitemporal Spatial Data by Deep Recurrent Neural Networks. *IEEE Geosci. Remote Sens. Lett.* **2017**, *14*, 1685–1689. [CrossRef]
50. Byeon, W.; Breuel, T.M.; Raue, F.; Liwicki, M. Scene labeling with lstm recurrent neural networks. In Proceedings of the IEEE Conference on Computer Vision and Pattern Recognition, Boston, MA, USA, 7–12 June 2015; pp. 3547–3555. [CrossRef]
51. Shen, Q.; Chen, Q.; Tang, B.-s.; Yeung, S.; Hu, Y.; Cheung, G. A system dynamics model for the sustainable land use planning and development. *Habitat Int.* **2009**, *33*, 15–25. [CrossRef]
52. Priyadarisini, K.D.; Umadevi, G. A System Dynamics Model for Assessing Land-Use Transport Interaction Scenarios in Chennai, India. *Sustainability* **2023**, *15*, 6297. [CrossRef]
53. He, C.; Shi, P.; Chen, J.; Li, X.; Pan, Y.; Li, J.; Li, Y.; Li, J. Developing land use scenario dynamics model by the integration of system dynamics model and cellular automata model. *Sci. China Ser. D Earth Sci.* **2005**, *48*, 1979–1989. [CrossRef]
54. Haghani, A.; Lee, S.Y.; Byun, J.H. A system dynamics approach to land use/transportation system performance modeling Part II: Application. *J. Adv. Transp.* **2003**, *37*, 43–82. [CrossRef]
55. Noviandi, N.; Pradono, P.; Tasrif, M.; Kusumantoro, I.P. Modeling of dynamics complexity of land use and transport in megapolitan urban fringe (case of Bekasi city). *Transp. Res. Procedia* **2017**, *25*, 3314–3332. [CrossRef]
56. He, J.; Li, X.; Liu, P.; Wu, X.; Zhang, J.; Zhang, D.; Liu, X.; Yao, Y. Accurate Estimation of the Proportion of Mixed Land Use at the Street-Block Level by Integrating High Spatial Resolution Images and Geospatial Big Data. *IEEE Trans. Geosci. Remote Sens.* **2021**, *59*, 6357–6370. [CrossRef]

Disclaimer/Publisher's Note: The statements, opinions and data contained in all publications are solely those of the individual author(s) and contributor(s) and not of MDPI and/or the editor(s). MDPI and/or the editor(s) disclaim responsibility for any injury to people or property resulting from any ideas, methods, instructions or products referred to in the content.